PEOPLE'S DEMOCRATIC REPUBLIC OF ALGERIA

Ministry of Higher Education and Scientific Research

University of Amar Telidji - Laghouat

Faculty of Technology

Department of Electronics

MASTER THESIS

DOMAIN: Science & Technology

FIELD: Electronic

SPECIALTY: Instrumentation

FEIDJEL Abderrahmane & BENSAFIDDINE Ahmed Nadir

Theme

Non-linear Controller to push PV system produce Maximum Power Point

Jury members:

HADJAISSA Aboubakeur	MCA	President
BENMILOUD Mohammed	MCB	Examiner
OUBBATI Brahim Khalil	MCB	Supervisor
ABOUCHABANA Nabil	MCB	Co-Supervisor

2022 / 2023

Abstract

This master's thesis focuses on the realization of a nonlinear control strategy aimed at achieving maximum energy extraction from photovoltaic (PV) modules. The aim of this work is to improve the performance and efficiency of photovoltaic systems by developing a control strategy that dynamically adjusts the point of operation of the photovoltaic module. It begins with an overview of solar energy and photovoltaic systems, providing a foundation for understanding the principles and components of photovoltaic technology. It also delves into the study of DC-DC converters and Maximum Power Point Tracking (MPPT) algorithms, highlighting their importance in extracting the maximum available power from a PV module. Extensive simulations of different MPPT algorithms have been performed to evaluate their effectiveness in maximizing energy production by the photovoltaic system. Finally, this Master thesis focused on the experimental implementation of the nonlinear controller. Real-world experiments are performed to verify the performance and feasibility of the proposed nonlinear control strategy. The experimental results demonstrate the practical application and effectiveness of the developed nonlinear controller algorithm in achieving the maximum energy extraction from the photovoltaic module.

Keywords: Integral Sliding Mode controller, PI regulator, photovoltaic, Maximum Power Point Tracking, Hill-Climbing, DC-DC converter.

Résumé

Ce mémoire de master porte sur la réalisation d'une stratégie de contrôle non linéaire visant à obtenir une extraction maximale d'énergie à partir de modules photovoltaïques (PV). L'objectif de ce travail est d'améliorer les performances et l'efficacité des systèmes photo-

voltaïques en développant une stratégie de contrôle qui ajuste dynamiquement le point de fonctionnement du module photovoltaïque. Il commence par un aperçu de l'énergie solaire et des systèmes photovoltaïques, fournissant une base pour comprendre les principes et les composants de la technologie photovoltaïque. Il se penche également sur l'étude des convertisseurs DC-DC et des algorithmes de suivi du Point de puissance Maximal (MPPT), soulignant leur importance pour extraire la puissance maximale disponible d'un module photovoltaïque. Des simulations approfondies de différents algorithmes MPPT ont été effectuées pour évaluer leur efficacité à maximiser la production d'énergie par le système photovoltaïque. Enfin, ce mémoire de master s'est concentré sur la mise en œuvre expérimentale du contrôleur non linéaire. Des expériences en conditions réelles sont effectuées pour vérifier la performance et la faisabilité de la stratégie de contrôle non linéaire proposée. Les résultats expérimentaux démontrent l'application pratique et l'efficacité de l'algorithme de contrôleur non linéaire développé pour obtenir l'extraction maximale d'énergie du module photovoltaïque.

mots-clés: Contrôleur intégral en mode glissant, régulateur PI, photovoltaïque, suivi du point de puissance maximale (MPPT), convertisseur DC-DC.

ملخص

تركز مذكرة الماستر هذه على تحقيق استراتيجية التحكم غير الخطية التي تهدف إلى تحقيق أقصى استخلاص للطاقة من الوحدات الكهروضوئية(PV). الهدف من هذا العمل هو تحسين أداء وكفاءة الأنظمة الكهروضوئية من خلال تطوير استراتيجية تحكم تضبط ديناميكيًا نقطة تشغيل حيث تبدأ بنظرة عامة على الطاقة الشمسية والأنظمة الكهروضوئية، مما يوفر أساسا لفهم مبادئ ومكونات تكنلوجيا الأنظمة الكهروضوئية. كما وتتعمق في دراسة محولات مستمر- مستمر وخوارزميات تتبع نقطة الطاقة القصوى (MPPT)، مع إبراز أهميتها في استخراج الحد الأقصى من الطاقة المتاحة من الوحدة الكهروضوئية. تم إجراء عمليات محاكات مكثفة للعديد من الخوارزميات MPPT لتقديم فعاليتها في تنظيم إنتاج الطاقة بواسطة النظام الكهروضوئي. أخيرا ركزت على التنفيذ التجريبي لوحدة التحكم غير المتدرجة. يتم إجراء تجارب واقعية للتحقق من أداء وجدوى استراتيجية التحكم غير الخطية المقترحة. توضح النتائج التجريبية التطبيق العملي وفعالية خوارزمية وحدة التحكم غير الخطية المطورة في تحقيق أقصى استخلاص للطاقة من الوحدة الكهروضوئية.

الكلمات المفتاحية: التحكم في وضع الانزلاق المتكامل ISMC، وحدة التحكم PI، تتبع نقطة الطاقة القصوى، محول مستمر-مستمر.

Acknowledgements

In the name of ALLAH, the Most Gracious and the Most Merciful

Thanks to ALLAH who is the source of all the knowledge in this world, for the strengths and guidance in completing this thesis. we express our deep sense of gratitude and heartfelt thanks first of all to our parents for their concern for us and for their hard work and spending on our behalf and our supervisor, Dr.OUBBATI Brahim Khalil, for his invaluable guidance, patience, kindness, and consistent encouragement throughout the course of this work. Also, we would like to thank, Dr. BENMILOUD Mohammed, ABOUCHABANA Nabil, and Dr.AMMER Khaled for their valuable input, encouragement, and intellectual stimulation.

We extend our appreciation to our families and friends for their unwavering support, patience, and understanding during this challenging journey. Their encouragement and believing in us have been a constant source of motivation.

Finally, we are thankful to all the individuals who have contributed to our education and personal growth, directly or indirectly. Their efforts have shaped my academic journey and helped me develop as a researcher.

This thesis would not have been possible without the collective support and encouragement from all these individuals, and for that, we are sincerely grateful."

Special thanks to LACoSERE and LTTS laboratories members. Their support and benefit discussions make the way to accomplish this work easy.

Contents

List of Figures

General Introduction

Solar energy has emerged as a promising renewable energy source, offering a sustainable and environmentally friendly alternative to traditional power generation methods. Photovoltaic (PV) systems, which harness sunlight to generate electricity, have gained significant attention due to their wide applicability and potential for clean energy production. Maximizing the power output of PV modules is critical to improving the overall efficiency and performance of PV systems. This goal is the primary focus of this thesis.

This master thesis is divided on four chapters besides the introduction and the conclusion:

- **In chapter one**, we will present an overview of solar energy and photovoltaic systems, exploring the basic principles of solar energy conversion and the components of a typical photovoltaic system. By understanding the fundamentals of solar energy and photovoltaic systems, we lay the foundation for further exploration in optimizing energy extraction.

- **The second chapter** delves into the world of DC-DC converters and Maximum Power Point Tracking (MPPT) algorithms. DC-DC converters play a vital role in PV systems, facilitating the efficient transfer of power between the PV module and the load or energy storage system. In addition, MPPT algorithms dynamically adjust the operating point of the photovoltaic system to ensure maximum energy extraction under different environmental conditions.

- **The third chapter** focuses on simulating different MPPT algorithms, with the aim of evaluating their performance in maximizing power output from the PV module.

Through simulations and detailed analysis, we gain valuable insights into the effectiveness and efficiency of different control strategies.

- **In the fourth chapter**, we test *experimental* implementation of the simulation results. By performing real-world experiments, we validate the performance of the proposed nonlinear control strategy to maximize the power from the photovoltaic module. The experimental section serves as a critical step in bridging the gap between simulation-based results and practical application.

  Basically, this thesis seeks to contribute to the advancement of photovoltaic system optimization by realizing a nonlinear control strategy. By enhancing the energy extraction capabilities of photovoltaic modules, we aim to harness the full potential of solar energy and pave the way for a more sustainable and efficient future.

Chapter 1

SOLAR ENERGY and PV SYSTEM

1.1 Introduction

One method of utilization of the solar deposit is the conversion of solar radiation into energy via the photovoltaic process. In a world where pollution and the greenhouse effect are threatening the environment, clean energy generation has become an absolute requirement. Photovoltaic (PV) is a renewable and inexhaustible source of electricity. It is an important component of renewable energies that can help the world fulfill its ever-increasing energy demands while limiting greenhouse gas emissions and decreasing pollution.

1.2 Solar energy

The sun delivers its energy to us in two main forms: heat and light. There are two main types of solar power systems, namely, solar thermal systems that trap heat to warm up water and solar PV systems that convert sunlight directly into electricity as shown in Figure 1.1. The word photovoltaic comes from "photo," meaning light, and "voltaic," which refers to producing electricity. And that's exactly what photovoltaic systems do turn light into electricity! Direct or diffuse light (usually sunlight) shining on the solar cells induces the photovoltaic effect, generating DC electric power. This DC power can be used, stored in a battery system, or fed into an inverter that converts

DC into alternating current "AC", so that it can feed into one of the building's AC distribution boards ("ACDB") without affecting the quality of power supply[1].

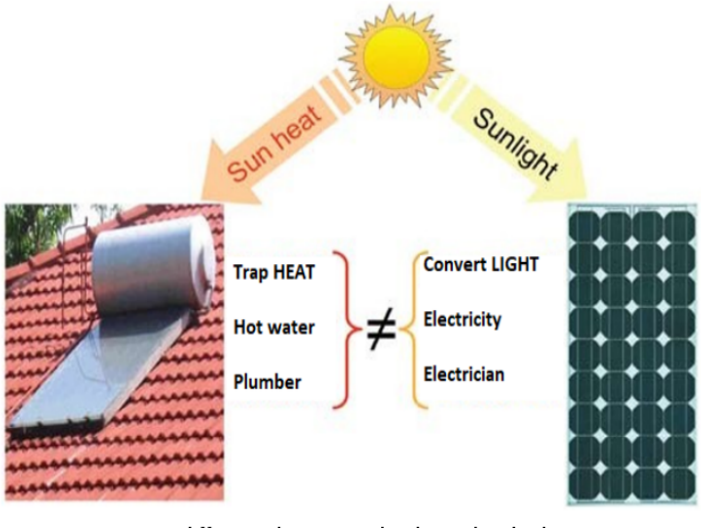

Figure 1.1: The sun heat and sun light

Important thing to note is that we are not concerned about the heat content of sunlight, *PV* cells and modules do not utilize the heat, only the light. When the source of light is not the sunlight then the photovoltaic cell is used as the photo detector. The example of the photo detector is the infra-red detectors[1].

1.2.1 Solar energy a sustainable alternative to fossil and nuclear fuels

Solar energy is emerging as a promising alternative to traditional energy sources, such as fossil fuels and nuclear energy. Solar energy is a clean, renewable source of energy that does not emit greenhouse gases or other pollutants that contribute to climate change. Unlike fossil fuels and nuclear energy, which are finite and non-renewable, solar energy is abundant and inexhaustible. With advances in technology, solar power systems are becoming increasingly affordable and efficient, making them a practical and cost-effective option for a range of applications, from small residential systems to large commercial facilities and utilities. As the world faces growing concerns about

Figure 1.2: Non-renewable Resource Fossil Fuel and Renewable Energy

climate change and the need to transition to sustainable energy sources, solar energy is likely to play an increasingly important role in meeting global energy needs[2].

1.2.2 The expected future of solar energy

The future of solar energy looks exceptionally promising as it continues to evolve and expand its global presence. According to the International Energy Agency, solar energy is set to become the largest source of electricity by 2050, surpassing all other conventional energy sources. This projection is supported by lower costs of solar technologies, increased efficiency of solar panels, favorable government policies that stimulate the adoption of renewable energy .

Moreover, continuous R'and'Defforts are focused on improving energy storage solutions to meet the challenges of intermittent power generation. As the world recognizes the urgent need to combat climate change and transition to sustainable energy sources, solar energy is in a position to play a pivotal role in meeting the growing energy demand while significantly reducing greenhouse gas emissions. Its ability to provide homes, businesses and entire communities with clean, reliable and affordable energy makes solar a key driver in the global energy transition towards a greener and more sustainable future.

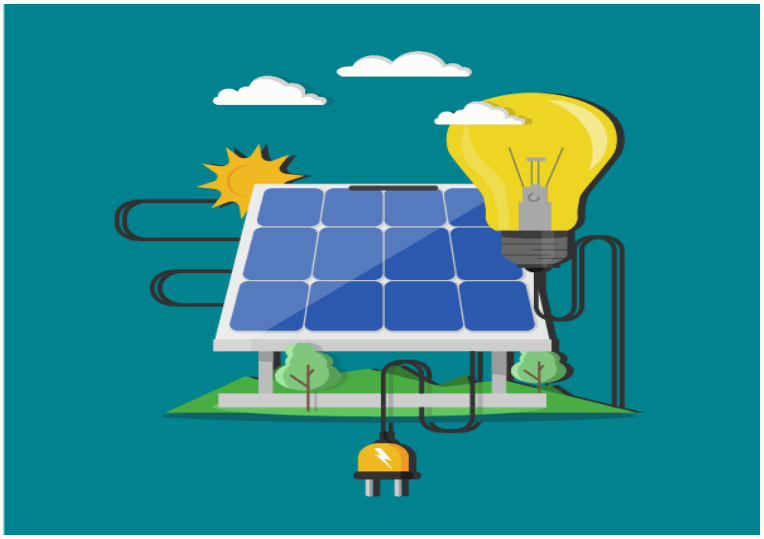

Figure 1.3: Solar power illustration

1.2.3 How to produce the solar energy

Solar energy is produced through the use of solar panels, which consist of photovoltaic (PV) cells. These cells convert sunlight into electricity using the photovoltaic effect. When sunlight hits cells, it causes electrons to escape from their atoms, causing electricity to flow. This electricity is then collected by wiring the cells together and sent to an inverter, which converts direct electric current (DC) produced by the cells into alternating current (AC) that can be used in homes and businesses. There are three main types of solar panels: monocrystalline, polycrystalline and thin film Monocrystalline look figure 1.4.

1.2.4 How these system work?

Solar panels harness the energy from the sun's photons to generate electricity through the photovoltaic effect. Although producing a relatively small amount of power individually, solar panels can be linked together in an array to generate larger amounts of power.

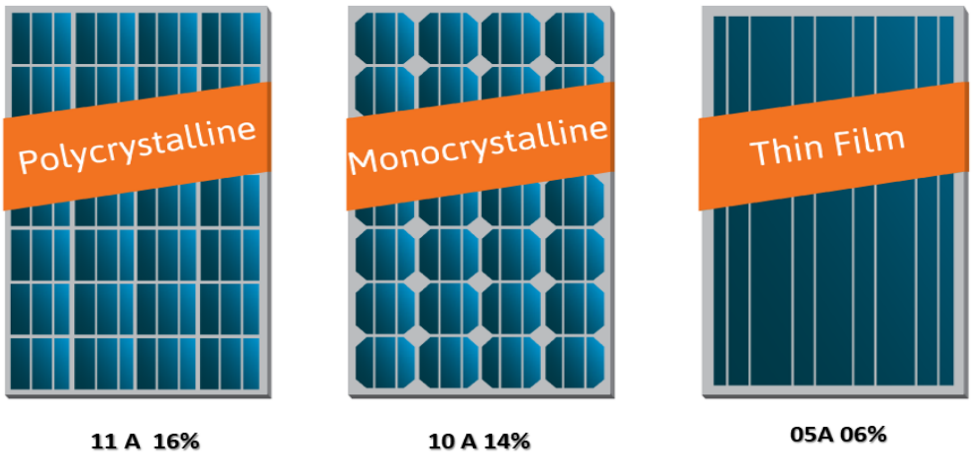

Figure 1.4: Type and efficiency of *PV*

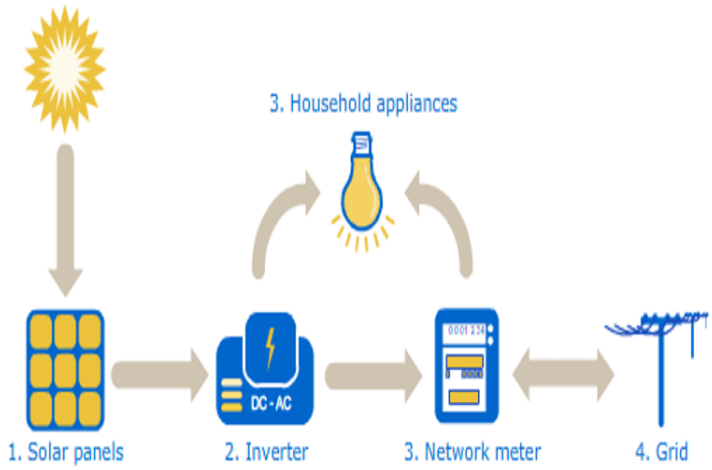

Figure 1.5: Residential grid-tied solar *PV* system diagram

The electrical current generated by a solar panel or array is in the form of direct current (DC), which must be converted to alternating current (AC) to be useful for powering electronic devices and for integration with the electrical grid. An inverter is used to convert direct current into alternating current, allowing solar energy to be used locally or transferred to the grid for use at other locations[3].

1.3 The history of the solar cells

Some important dates in the history of photovoltaics:

1839: French physicist Edmond Becquerel discovers the process of using sunlight to produce electric current in a solid material. This is the photovoltaic effect.

1875: Werner Von Siemens exposes in front of the Academy of Sciences of Berlin an article on the photovoltaic effect in the semiconductors. But until the Second World War, the phenomenon was still a laboratory curiosity.

1954: Three American researchers, Chapin, Pearson and Prince, are developing a high-efficiency photovoltaic cell at a time when the emerging space industry is looking for new solutions to power its satellites.

1958: A cell with a yield of 9 is developed. The first satellites powered by solar cells are sent into space.

1973: The first house powered by photovoltaic cells is built at the University of Delaware.

1983: The first car powered by photovoltaic energy travels a distance of 4000 km in Australia [4].

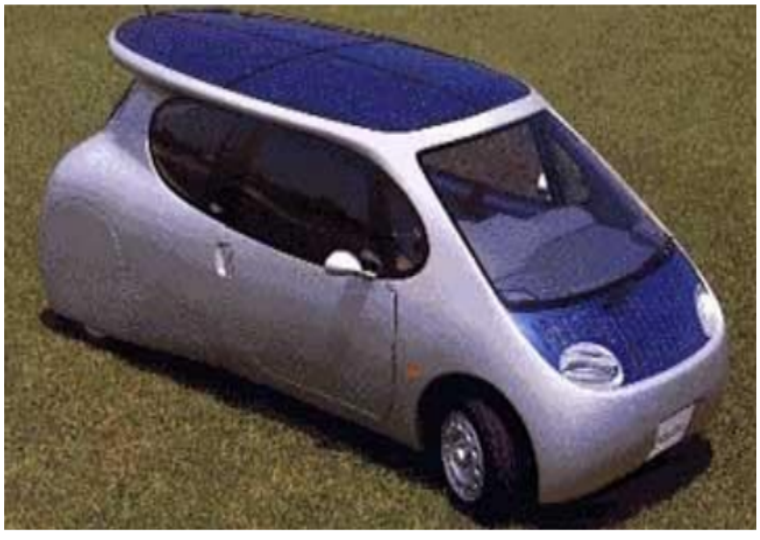

Figure 1.6: The first car powered by photovoltaic energy

1.4 The photovoltaic effect

The photovoltaic effect is a phenomenon in which certain materials, such as silicon, generate an electric current when they are exposed to light. This effect is the basis for the operation of solar cells, which convert sunlight directly into electricity. When light strikes the surface of a solar cell, it excites electrons in the material, causing them to flow through an external circuit and produce electrical power.

1.5 The photovoltaic cell

1.5.1 Definition of the photovoltaic cell

A photovoltaic cell, or solar cell, is an electronic component which, exposed to light, produces electricity through the photovoltaic effect. The power obtained is proportional to the incident light power and depends on the efficiency of the cell. This delivers a DC voltage and a current passes through it as soon as it is connected to an electrical load (usually an inverter, sometimes a simple electric battery)[5].

1.5.2 Photovoltaic cell principle of operation

The utilization of the photovoltaic effect in solar cells allows for the direct conversion of sunlight into electricity by generating and transporting positive and negative electric charges in a semiconductor material, under the influence of light. This material comprises of two sections, namely n-type doped and p-type doped, with one section possessing an excess of electrons and the other section having a deficit of electrons, respectively. When these two sections are brought into contact, electrons from the n-type material diffuse into the p-type material, causing the initially n-doped area to become positively charged, and the initially p-doped area to become negatively charged. This creates an electric field between them, which pushes back the electrons in the n zone and the holes towards the p zone, leading to the formation of a junction (known as p-n). By adding metal contacts on the n and p regions, a diode is produced[6].

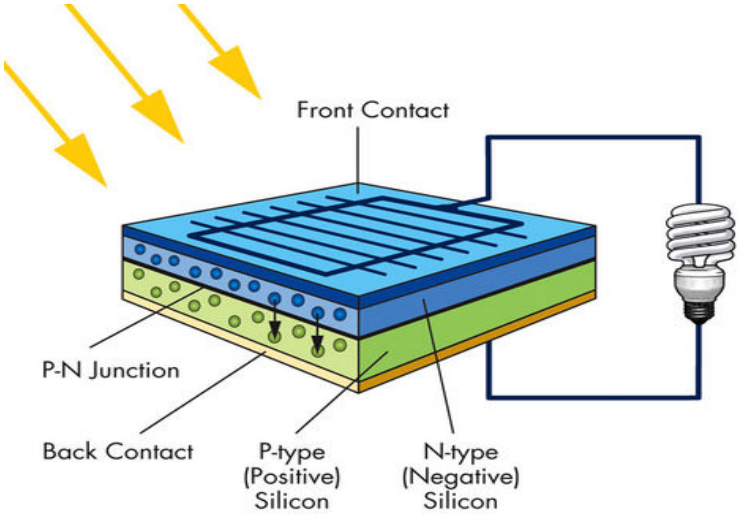

Figure 1.7: How solar cells work

Electrons move solely from the p zone to n, while holes move from n to p. This movement is made possible by the use of a semiconductor material. When the junction is exposed to light, photons with an energy equal to or greater than the width of the forbidden band impart energy to the atoms, causing each of them to release an electron from the valence band into the conduction band, leaving behind a hole. This process generates an electron-hole pair. If a charge is applied to the terminals of the cell, the electrons from the n zone combine with the holes from the p zone through the external connection, leading to a potential difference, which allows the electric current to flow[6].

1.6 Solar Cell and Modeling

The photovoltaic cell is formed by a semiconductor material of the P-N type. The size of each cell ranges from a few square centimeters up to $100cm^2$ or more. Its shape is circular, square or derived from the two geometries (Figure 1.8) [7].

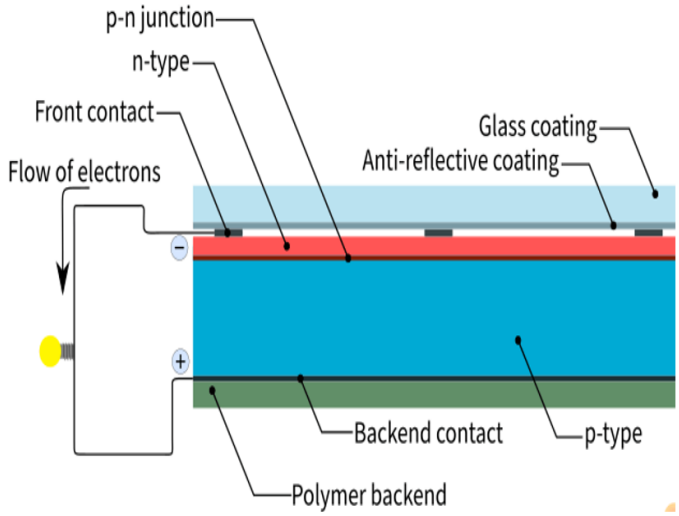

Figure 1.8: Cross section of a typical PV cell

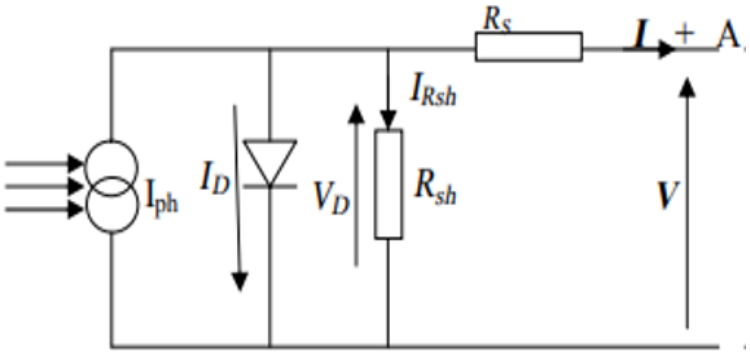

Figure 1.9: Equivalent diagram of a solar cell

The maximum cell voltage is around 0.6V for zero current. This voltage is called the open circuit voltage(V_{oc}) . The maximum current occurs when the terminals of the cell are short-circuited, it is called short-circuit current (I_{sc}) and is highly dependent on the level of illumination. A PV cell has, as we see in figure 1.11, a nonlinear characteristic I = f(v)

Therefore , a PV cell made up of a silicon-based PN junction can be modeled by the following equation:

$$I = Iph - ID - Ish \tag{1.1}$$

$$I = I_{ph} - I_S \left[\exp\left(q \frac{V + R_S I}{AKT} \right) - 1 \right] - \frac{V + R_S I}{R_{Sh}} \tag{1.2}$$

$$V_{th} = \frac{AKT}{q} \tag{1.3}$$

Where:

- I_{ph}: The photo-current.
- q: The charge of the electron $= 1,6 * 10^{-19}$C.
- I: The current generated by the solar cell.
- A: The quality factor of the cell.
- V: The voltage at the terminals of the cell.
- K: The boltzmanne constant $= 1.38 * 10^{-23} J/K$
- R_s: The series resistance.
- T: The operating temperature in Kelvin.
- R_{sh}: The shunt resistance.
- V_{th}: Thermal tension.
- I_s: The saturation current.

Five parameters must be evaluated, whatever the lighting and temperature conditions, they are: R_s,I_s,R_{sh},I_{ph},V_{th}.

Depending on the recombination mechanisms, cell A's quality factor ranges from 1 to 2 for amorphous cells and equals 2 for crystalline cells. For high currents, it is roughly 1, and for low currents, it rises to 2 [8].

The resistance R_{sh} is a result of recombination losses brought on by thickness, surface effects, and junction non-ideally. Since this resistance (of the order of the mega Ohm) is much higher in actual use than the series resistance, its impact is disregarded. The simplified equivalent electrical circuit as a consequence is depicted in the figure below(1.10):

So the original equation of (1.2) becomes :

$$I = I_{ph} - I_S \left[\exp\left(q\frac{V + R_S I}{AKT}\right) - 1\right] \tag{1.4}$$

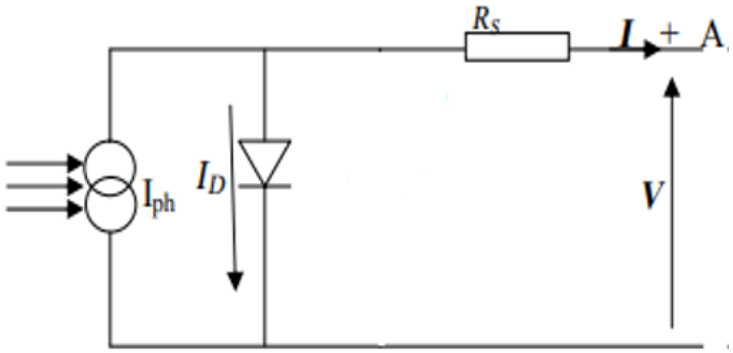

Figure 1.10: Simplified equivalent diagram of a real solar cell connected to a load

We have I = f(v) and P = f(v) are *non*-linear characteristics of a *PV* cell, When the PV cell's electrical model is used, the Math works MATLAB environment can simulate the *PV* cell's activity.

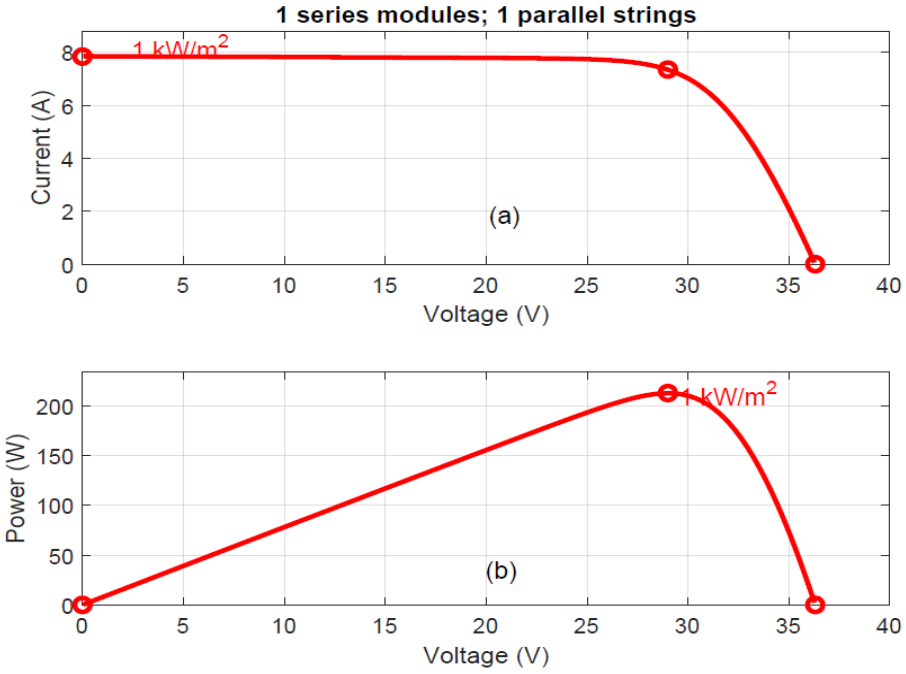

Figure 1.11: *PV* system characteristics a) (P-V)characteristic, b) (I-V) characteristic

1.6.1 The series resistance R_s

The series resistance R_s stands in for the different contact and connection resistances, and it is mostly caused by Joule effect losses through the collection gates, the intrinsic

resistance of semiconductors, as well as faulty connections (semiconductor, electrodes). In reality, the series resistance R_s is relatively low (on the scale of a few Millie-ohms), but it has a significant impact on the slope of the curve (I-V) in an open circuit[7].

$$Rs = -\left.\frac{dV}{dI}\right|_{Voc,0} - \frac{1}{X_V} \tag{1.5}$$

$$X_V = \frac{I_{S,0}}{V_{th,0}} e^{\frac{Voc,0}{V_{th,0}}}. \tag{1.6}$$

1.6.2 Short circuit current I_{sc}

The short-circuit current is the current through the solar cell when the voltage across the solar cell is zero (i.e., when the solar cell is short circuited). Usually written as I_{sc}, the short-circuit current is shown on the IV curve below.[9]

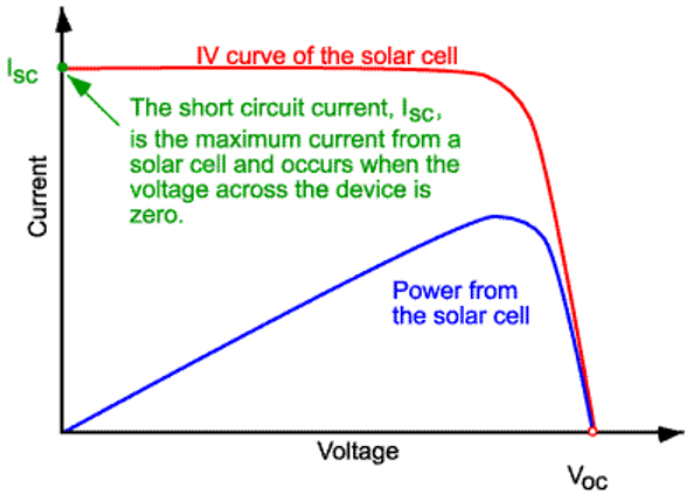

Figure 1.12: Curve of a solar cell showing the short-circuit current

In the ideal case (null and R_{sh} infinite), this current merges with the current photo I_{ph}

$$I_{sh} = I_{ph} \tag{1.7}$$

Alternatively, by negating the voltage V in equation (1.2), we get:

$$I_{Sc} = I_{ph} - I_0 \left(e^{q\left(\frac{R_S I_{SC}}{nKT}\right)} - 1 \right) - \frac{I_{Sc} R_S}{R_p} \tag{1.8}$$

1.6.3 The open circuit voltage V_{oc}

The open-circuit voltage,V_{oc} is the maximum voltage available from a solar cell, and this occurs at zero current. This voltage hardly varies with the light intensity is called open circuit voltage V_{oc}.

An equation for V_{oc} is found by setting the net current equal to zero in the solar cell equation to give:

$$V_{oc} = \frac{AkT}{q} \operatorname{In}\left(\frac{I_{ph}}{l_s} + 1\right) = V_{th} \operatorname{In}\left(\frac{I_{ph}}{l_s} + 1\right) \tag{1.9}$$

1.6.4 The efficiency η

The most widely used parameter to comparing the performance of one solar cell to another is efficiency. which is defined as the ratio of the maximum power provided by the cell P_{max} to the power of incident solar radiation P_{in} in is a critical characteristic for photovoltaic components[9].

The efficiency of a solar cell is determined as the fraction of incident power which is converted to electricity and is defined as:

$$P_{\max} = V_{OC} I_{SC} FF \tag{1.10}$$

$$\eta = \frac{V_{OC} I_{SC} FF}{P_{in}} \tag{1.11}$$

Where:

- V_{oc} is the open-circuit voltage;
- I_{sc} is the short-circuit current;
- FF is the fill factor
- η is the efficiency.

Several factors influence the performance of solar panels, including: Sunlight availability, temperature, shading and panel orientation. . . .etc.

1.7 Association of photovoltaic modules

Photovoltaic (PV) module association refers to how many PV modules are linked together to form a bigger PV array. The manner in which the modules are connected influences the array's electrical output, and hence the overall efficiency and performance of the PV system. PV modules may be connected in two ways: in series and in parallel.

1.7.1 Series association

The individual cell, the basic unit of a photovoltaic system, only produces a very low electrical power, typically 0.5 W with a voltage of less than one volt. To produce more power, the cells are assembled to form a module (or panel). In a series association, the positive terminal of one PV module is connected to the negative terminal of the next module, and so on, to form a chain.

The series association of the cells delivers a voltage equal to the sum of the individual voltages and a current equal to that of a single cell[4].

$$V_{ocNS} = N_S \times V_{oc} \tag{1.12}$$

$$I_{scNS} = I_{sc} \tag{1.13}$$

- $V_{oc}NS$: The sum of the open circuit voltages of NS cells in series.
- $I_{sc}NS$: The short-circuit current of NS cells in series.

1.7.2 Parallel association

In a parallel association, the positive terminals of all the PV modules are connected together, as are the negative terminals. The resulting voltage does not change but the resulting intensity is the sum of the intensities of each module Parallel association is typically used when the current required by the load is higher than that of a single module[9].

$$I_{scNP} = N_P \times I_{sc} \tag{1.14}$$

$$V_{oc} = V_{ocNP} \tag{1.15}$$

– $I_{sc}NP$: The sum of the cost circuit currents of (NP) cell in parallel.

– $V_{oc}NP$: The open circuit voltage of (NP) cells in parallel.

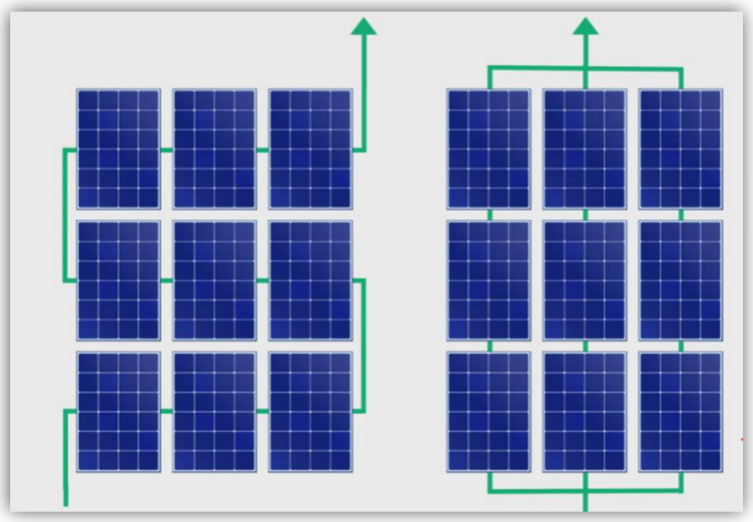

Figure 1.13: Connection of Solar Panels in Series and parallel

$$P_{\text{generator}} = N_{ms} \cdot N_{BP} \cdot P_{\text{module}} \tag{1.16}$$

$$V_{\text{generator}} = N_{ms} \cdot V_{\text{module}} \tag{1.17}$$

$$I_{\text{generator}} = N_{BP} \cdot I_{\text{module}} \tag{1.18}$$

$$R_{\text{s generator}} = R_{s\ \text{module}} \cdot \frac{N_{ms}}{N_{BP}} \tag{1.19}$$

N_{ms}: Number of modules associated in series.

N_{BP}: Number of parallel branches.

1.8 Weather conditions influence

1.8.1 The irradiation influence

The current produced by the photocell $I_{ph}$is practically proportional to the solar illumination. on the other hand, the voltage V at the terminals of the junction varies little because it is a function of the potential difference at the P-N junction of the

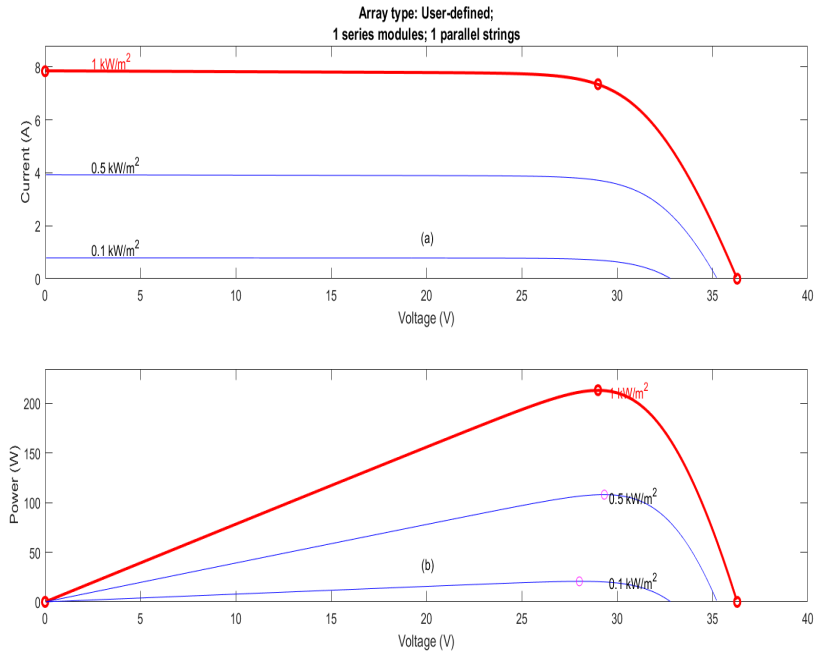

Figure 1.14: a) The irradiation influence with (P-V)characteristic, b) The irradiation influence with (I-V) characteristic

material itself. At a constant temperature, it is observed that the current undergoes a significant variation, but on the other hand the voltage varies slightly. Because the short-circuit current is a linear function of the illumination while the open circuit voltage is a logarithmic function[10, 11].

The open circuit voltage will only decrease slightly with the luminous flux. This therefore implies that :

- The optimal power of the cell (P_m) is practically proportional to the illumination.
- The maximum power points are located at approximately the same voltage (see figure 1.14)

1.8.2 The temperature influence

The temperature is an important parameter in the behavior of a solar cell, exposed to an irradiation of $1000w/m^2$ it transforms only 12% into electricity. It is essential to understand the effect of changing the temperature of a solar cell on the characteristic

$I = F(V)$. The current depends on the temperature since the current increases slightly as the temperature increases, but the temperature negatively affects the voltage of the circuit opens. As the temperature increases the open circuit voltage decreases. Consequently the maximum power of the generator undergoes a decrease [10].

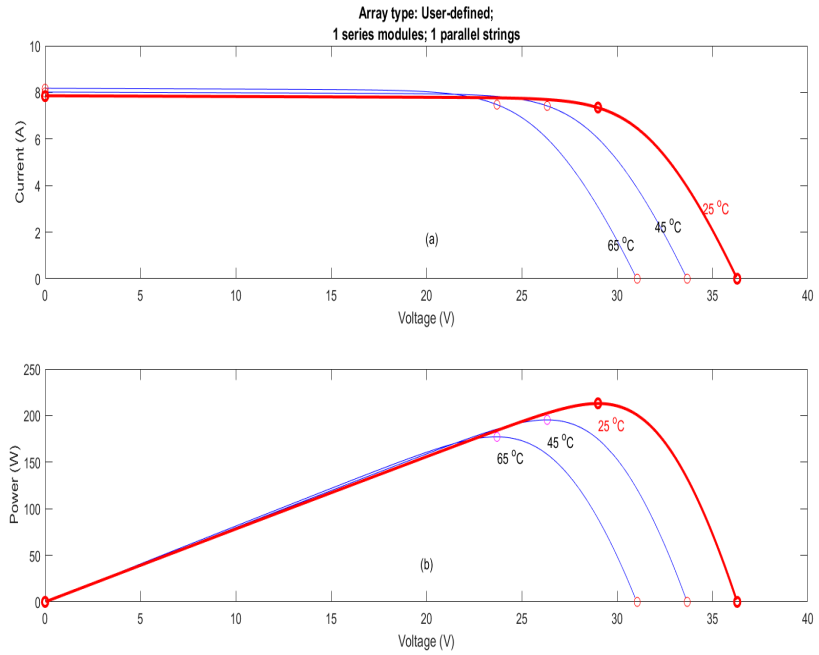

Figure 1.15: a) The temperature influence with (P-V)characteristic, b) The temperature influence with (I-V) characteristic

The figure 1.15 shows the influence of temperature on the current-voltage characteristic of the cell. When the temperature rises, the current increases while the voltage decreases, this results in a decrease in power.

1.8.3 The advantages and disadvantages of the photovoltaic systems

1.8.4 Advantages:

- Durability: As the source of the sun is not implemented.
- Saves you from paying the electricity bill.

- Their systems can be installed above surfaces because there is no space for their installation.
- The solar panel has a long service life and comes with a 25-year warranty.
- No pollution, no noise.
- In space applications, solar energy is the source of electrical energy.
- The sun is the hope of some remote regions in electricity[12].

1.8.5 Disadvantages :

- Intermittent: since in the presence of the sun there is energy, and in the night there is no energy.
- The cost of building electrical systems is very high.
- Solar panels must be constantly clean and free of dust and plankton in order to operate efficiently.
- In areas with heavy rains, the efficiency of energy systems is relatively low[12].

1.9 Assessment of renewable energy in Algeria

The Algeria initiates a dynamic green energy by launching an ambitious program of development of renewable energy and energy efficiency.

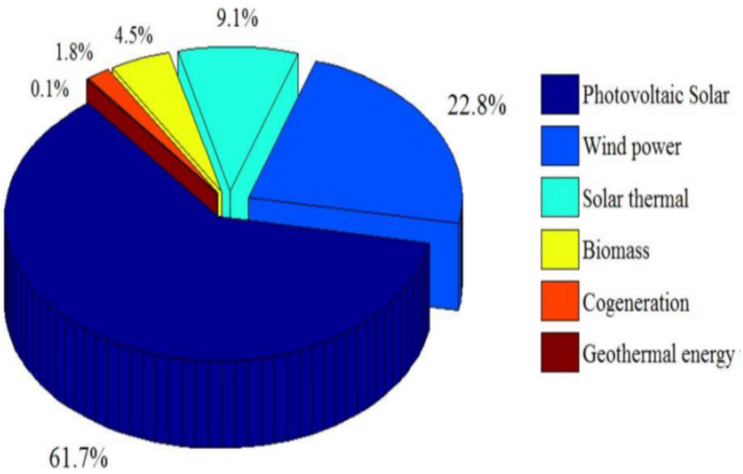

Figure 1.16: Distribution of development program of renewable energy technology sector

This vision of the Algerian government relies on a strategy focused on the development of inexhaustible resources such as solar and using them to diversify energy sources and prepare for the Algeria of tomorrow (Figure 1.16). The program adopted in 2011 for an overall objective consists in the installation of 22,000 MW by 2030, of which 10,000 MW could be dedicated to export[13].

1.9.1 Solar potential

In all Mediterranean basins, there is a gigantic reservoir of solar energy in the north of Africa and particularly the southern region of Algeria. The potential of this type of energy in southern Algeria is the largest .

The sunshine duration of almost all the national territory exceeds $2000h$ annually and reaches $3900h$ (high plains and Sahara). The energy received daily on a horizontal surface of $1m^2$ is about $5KWh$ over most of the country, or nearly $1700kWh/m^2/year$ in the north and 2263 $kWh/m^2/year$ in the south[14].

Region	Coastal	Highlands	Sahara
Area (%)	4	10	86
Average sun hours per year	2650	3000	3500
Energy received KWh/m2/year	1700	1900	2650

Table 1.1: Data on solar radiation in Algeria

1.10 Conclusion

This chapter, divided into two parts, allowed us first of all to define the different sources of global energy; namely renewable and non-renewable energies considering that solar energy is the energy of the future.

Secondly, we presented an overview of photovoltaic energy, the operating principle of a photovoltaic cell, and the use of its current-voltage characteristic to calculate its various physical parameters. We have also seen the effect of climate change on the I = f(v) characteristic of the GPV. In addition, its operating point depends on the load it supplies.

In order to extract the maximum power available at the terminals of the GPV at all times, we introduce an adaptation stage between the generator and the load, hence the aim of the second chapter.

Chapter 2

DC/DC converters and *MPPT* algorithms

2.1 Introduction

The previous chapter provided an overview of the current state of the art in PV systems. In this chapter, our primary emphasis was on examining the various types of Maximum Power Point Tracking (MPPT) controllers, encompassing both unconventional and conventional strategies, that can be employed in PV systems. It is worth noting that the magnitude of power generated by the PV system is significantly influenced by changing weather conditions, including temperature and solar irradiation. Therefore, the term MPPT refers to the Maximum Power Point Tracking controller, which plays a crucial role in optimizing a PV system to operate at its maximum power point [6, 15].

2.2 DC/DC converters

The chopper is a DC/DC converter for converting energy continuous at one level of voltage (or current) into continuous energy at another level of voltage (or current). Its use is necessary to store energy photovoltaic in batteries [6, 15].

Within the category of DC/DC converters, our concentration will be on a specific kind known as boost converter (parallel chopper).

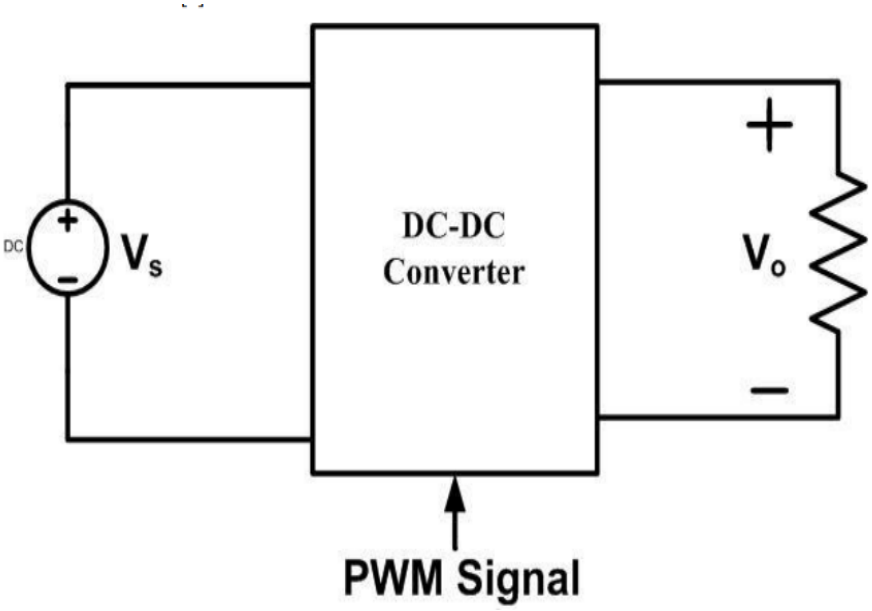

Figure 2.1: Schematic diagram of DC to DC conversion (DC-DC)

2.3 Boost converter

The main function of this converter is to deliver an output voltage greater than the input voltage, it is a voltage booster, it is also called parallel chopper, and its scheme is given by figure 2.2

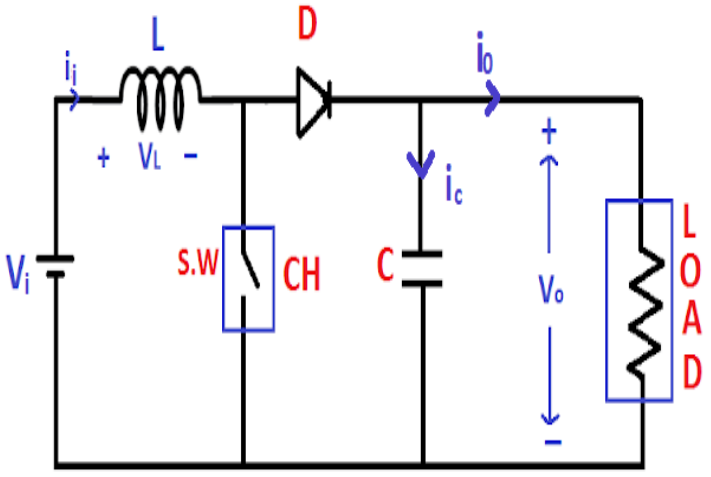

Figure 2.2: Boost converter

The circuit is powered by a voltage source V_i, the output is loaded by a resistor R and outputs a current I_i. Switch K, symbolized here as a power $MOSFET$, is a

periodically rendered conductor with a duty cycle α the frequency $F = 1/T$. There are two modes of operation of this circuit depending on whether the current flowing in the inductance L is or is not continuous (does not cancel during the period).

The continuous conduction mode being the most interesting for this converter, We will only study this mode.

K: Switch Function

- K= 1 The transistor is on — charging step
- K = 0 Transistor is off — diode on, discharge stage

When switch K is in the on state, the current in the boost inductor increases linearly and diode D is turned off at this time. When switch K is turned off, the energy stored in the inductor is released through the diode to the output RC circuit, The converter wave forms in the CCM are presented in Figure 2.3

The boost converter are operating in CCM, that's mean the inductor current never reaches to zero.

We have the boost converter circuits with two modes of switching ON and OFF .

Mode I : Switch is ON, Diode is OFF:

For the first period $(0 < t < DT)$: Switch K is closed, diode is off.

$$\begin{cases} i_c(t) = C\frac{dv0(t)}{dt} = -i_0(t) \\ V_L(t) = L\frac{diL(t)}{dt} = -V_i(t) \end{cases} \tag{2.1}$$

By applying Kirchhoff's laws to the circuit, we have the following two differential equations:

$$\begin{cases} -L\dot{x}_1(t) + u(t) = 0 \\ x_2 + CR\dot{x}_2 = 0 \end{cases} \tag{2.2}$$

We take the state variables such that:

$$\begin{cases} x_1(t) = i_L(t) \\ x_2(t) = v_C(t) \end{cases} \Rightarrow \begin{cases} \dot{x}_1(t) = 0x_1(t) + 0x_2(t) + \frac{1}{L}u(t) \\ \dot{x}_2(t) = 0x_1(t) - \frac{1}{CR}x_2(t) \end{cases} \tag{2.3}$$

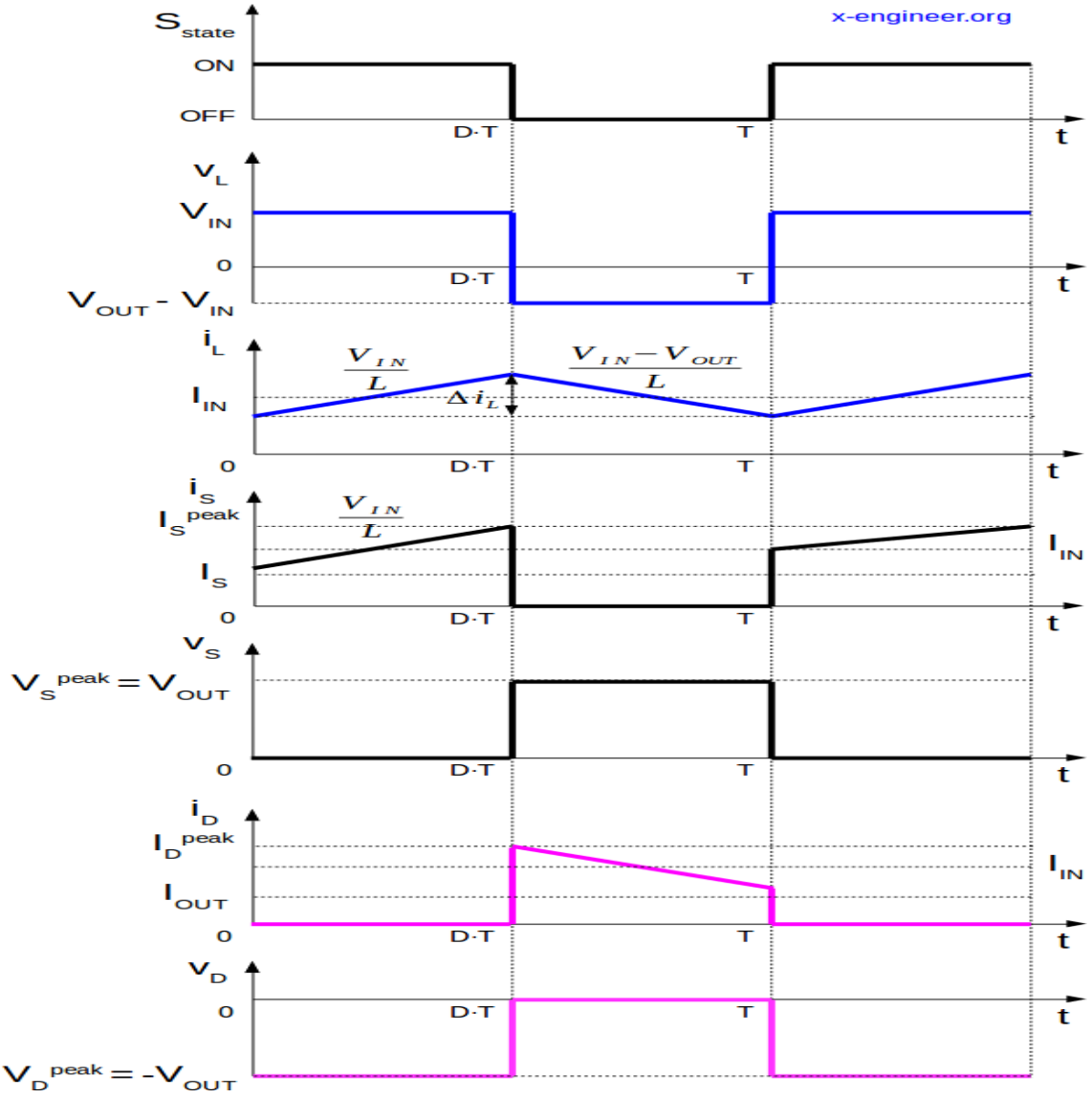

Figure 2.3: Wave forms of the boost converter

The output equation is:

$$\begin{aligned} y(t) = V_0(t) &\Rightarrow y(t) = Ri_0(t) \\ &\Rightarrow y(t) = CR\dot{x}_2(t) \\ &\Rightarrow y(t) = x_2(t) \end{aligned} \tag{2.4}$$

We can represent the system for the first subinterval as a state space using formula

$$\begin{cases} \dot{x}(t) = A_1 x(t) + B_1 u(t) \\ y(t) = C_1 x(t) \end{cases} \tag{2.5}$$

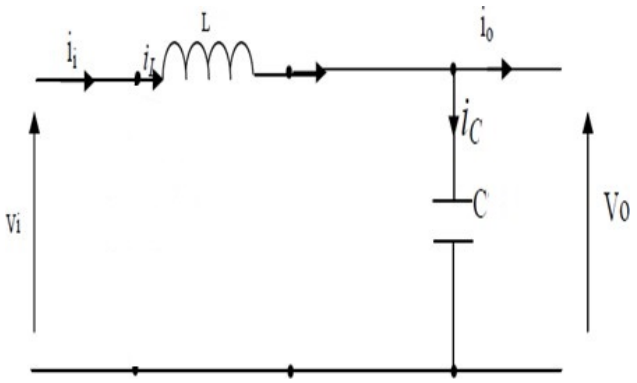

(a) Boost converter mode I.

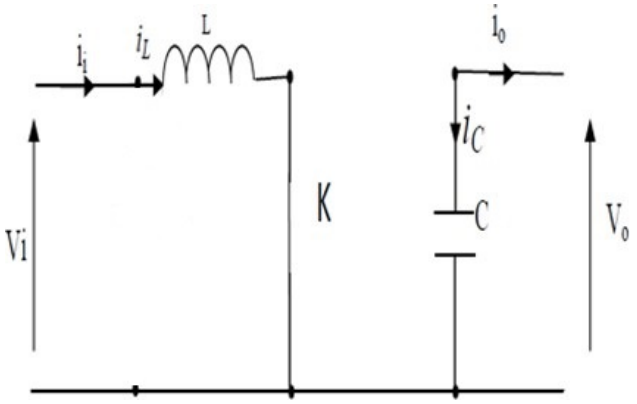

(b) Boost converter mode II .

Figure 2.4: Equivalent diagrams of the booster chopper, (a): K closed, (b): K open.

Such as :

$$A_1 = \begin{bmatrix} 0 & 0 \\ 0 & -\frac{1}{CR} \end{bmatrix}, B_1 = \begin{bmatrix} \frac{1}{L} \\ 0 \end{bmatrix} \text{ and } C_1 = \begin{bmatrix} 0 & 1 \end{bmatrix} \tag{2.6}$$

The representation of the system is as follows:

$$\begin{aligned} \begin{bmatrix} \dot{x}_1(t) \\ \dot{x}_2(t) \end{bmatrix} &= \begin{bmatrix} 0 & 0 \\ 0 & -\frac{1}{CR} \end{bmatrix} \begin{bmatrix} x_1(t) \\ x_2(t) \end{bmatrix} + \begin{bmatrix} \frac{1}{L} \\ 0 \end{bmatrix} u(t) \\ y(t) &= \begin{bmatrix} 0 & 1 \end{bmatrix} \begin{bmatrix} x_1(t) \\ x_2(t) \end{bmatrix} \end{aligned} \tag{2.7}$$

Mode II: Switch is OFF, Diode is ON:

For the second period $(DT < t < T)$: Switch K is open, diode is on.

$$\begin{cases} i_c(t) = C\frac{dv0(t)}{dt} = i_L(t) - i_0(t) \\ V_L(t) = L\frac{diL(t)}{dt} = V_i(t) - V_0(t) \end{cases} \tag{2.8}$$

The differential equations of the electrical diagram of the boost converter in the second continuous mode:

$$\begin{cases} -L\dot{x}_1(t) - x_2(t) + u(t) = 0 \\ x_2(t) - Ri_0(t) = 0 \end{cases} \tag{2.9}$$

According to the law of knots, we have the following equation:

$$i_L(t) = i_C(t) + i_0(t) \tag{2.10}$$

from where:

$$\begin{aligned} x_1(t) &= C\dot{x}_2(t) + i_0(t) \\ i_0(t) &= x_1(t) - C\dot{x}_2(t) \end{aligned} \tag{2.11}$$

Injecting equation ((2.12))into the system of equations ((2.13)).

$$\begin{cases} -L\dot{x}_1(t) - x_2(t) + u(t) = 0 \\ x_2(t) - R\left[x_1(t) - C\dot{x}_2(t)\right] = 0 \end{cases} \tag{2.12}$$

$$\begin{cases} \dot{x}_1(t) = -\frac{1}{L}x_2(t) + \frac{1}{L}u(t) \\ \dot{x}_2(t) = \frac{1}{C}x_1(t) - \frac{1}{CR}x_2(t) \end{cases} \tag{2.13}$$

The output equation is:

$$\begin{aligned} y(t) &= Ri_0(t) = R\left[x_1(t) - C\dot{x}_2(t)\right] \\ y(t) &= x_2(t) \end{aligned} \tag{2.14}$$

We can represent the system for the second interval as a state space as follows:

$$\begin{cases} \dot{x}(t) = A_2x(t) + B \\ y(t) = C_2x(t) \end{cases} \tag{2.15}$$

Such as :

$$A_2 = \begin{bmatrix} 0 & -\frac{1}{L} \\ \frac{1}{C} & -\frac{1}{CR_{ch}} \end{bmatrix}, B_2 = \begin{bmatrix} \frac{1}{L} \\ 0 \end{bmatrix} \text{ and } C_2 = \begin{bmatrix} 0 & 1 \end{bmatrix} \tag{2.16}$$

Hence its representation in state space is given as follows:

$$\begin{aligned} \begin{bmatrix} \dot{x}_1(t) \\ \dot{x}_2(t) \end{bmatrix} &= \begin{bmatrix} 0 & -\frac{1}{L} \\ \frac{1}{C} & -\frac{1}{CR} \end{bmatrix} \begin{bmatrix} x_1(t) \\ x_2(t) \end{bmatrix} + \begin{bmatrix} \frac{1}{L} \\ 0 \end{bmatrix} u(t) \\ y(t) &= \begin{bmatrix} 0 & 1 \end{bmatrix} \begin{bmatrix} x_1(t) \\ x_2(t) \end{bmatrix} \end{aligned} \tag{2.17}$$

We want to link the two state spaces, (A1, B1) for the interval [0, Ton], and (A2, B2) for the interval $[Ton, Toff]$.

To find a dynamic representation valid for the whole period T_s, we use usually the following expression [16]:

$$\left(\frac{dx}{dt}\right) T_s = \frac{dx}{dt_{D \cdot T_s}} d \cdot T_s + \frac{dx}{dt_{(1-D)T_s}} (1-d) \cdot T_s \tag{2.18}$$

By applying the relation (2.3) on the systems of equations (2.1) and (2.2), we obtain the equations that govern the system over an entire period:

$$\begin{cases} i_0(t) = (1-d) i_L(t) - C \frac{dv_0(t)}{dt} \\ V_i(t) = L \frac{di_L(t)}{dt} + (1-d) V_0(t) \end{cases} \tag{2.19}$$

The average model of the boost converter can be described by the state shape:

$$\begin{bmatrix} \frac{di}{dt} \\ \frac{dv}{dt} \end{bmatrix} = \begin{bmatrix} 0 & -\frac{(1-d)}{L} \\ -\frac{(1-d)}{C} & -\frac{1}{RC} \end{bmatrix} \begin{bmatrix} i \\ v \end{bmatrix} + \begin{bmatrix} -\frac{1}{L} \\ 0 \end{bmatrix} u_{(t)} \tag{2.20}$$

From which the DC voltage transfer function turns out to be

$$M_V = \frac{V_0}{Vs} = \frac{1}{1-D} \tag{2.21}$$

As the name of the converter suggests, the output voltage is always higher than the input voltage.

The up converter works in the CCM for $L > L_b$ where

$$L_b = \frac{(1-D) 2D \cdot R}{2 \cdot f} \tag{2.22}$$

As shown in Figure 2.3, the current supplied to the output RC circuit is discontinuous.Thus, a larger filter capacitor is required compared to that of derivative converters step-down to limit output voltage ripple. The filter capacitor must provide the DC output current to the load when diode D is off. The minimum value of the capacitance of the filter which results in the voltage ripple V is given by

$$C_{\min} = \frac{DV_0}{V_r R_f} \tag{2.23}$$

2.4 Maximum power point algorithms

The simplest conceivable installation consists of a field photovoltaic, formed by one or more modules connected in series or in parallel, and a load (resistive load or battery) which directly uses the energy produced (Figure 2.5). This installation provides a useful effect only during sunny periods and for temperatures well defined.

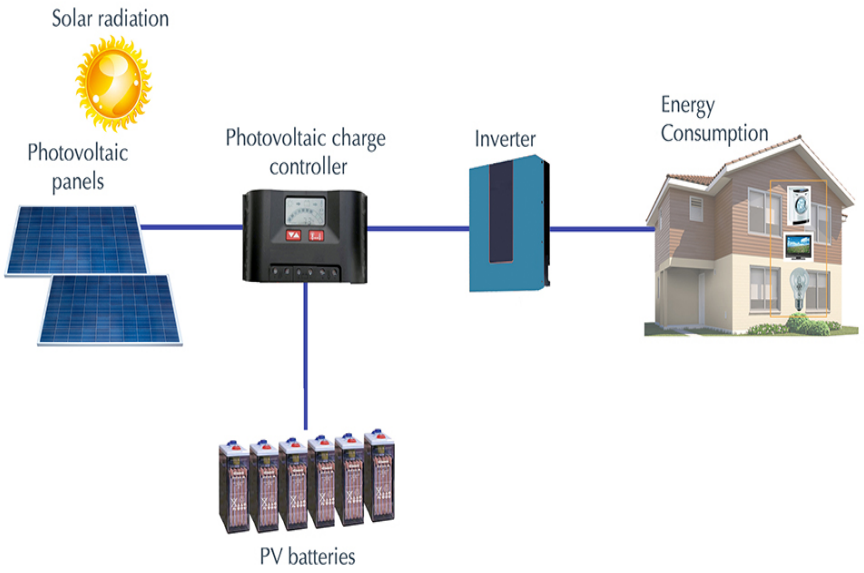

Figure 2.5: Photovoltaic installation

The current supplied to the load strongly depends on the intensity of the illumination for a given temperature and the nature of the load [17].

2.4.1 MPPT Principle work

The MPPT (Maximum Power Point Tracking) control plays a vital role in optimizing the performance of a *PV* system by finding the optimal operating point of the *PV* generator, which is influenced by weather conditions and load variations [15]. The principle of MPPT regulation involves automatically adjusting the duty cycle (D) to ensure continuous maximization of power output from the *PV* array.

The objective is to design and implement a digital controller that allows the optimal power generated by the solar panel to be efficiently transferred to the load, regardless

of variations in illumination intensity or load value.

For instance, when the incident power is $W1$, the maximum power transferred to the load can only be achieved at a specific duty cycle, α1opt (PPM1 point on Figure 2.6a). If the incident power changes to W2, the maximum power point shifts to PPM2, requiring the adjustment of the duty cycle toα2opt for the system to converge to the new optimal operating point.

Similarly, when the load resistance (RS) changes (Figure 2.6b), the maximum power point deviates from its optimal position (PPM1). To converge back to PPM1, the duty cycle α needs to be adjusted. In an independent and autonomous PV system, this regulation process must occur automatically to maintain optimal operation.The MPPT command is responsible for carrying out this regulation in practice. It ensures that the duty cycle is adjusted dynamically to track the maximum power point and optimize the power transfer from the solar panel to the load. By continuously monitoring and adjusting the duty cycle, the MPPT control ensures efficient operation of the PV system under varying conditions.

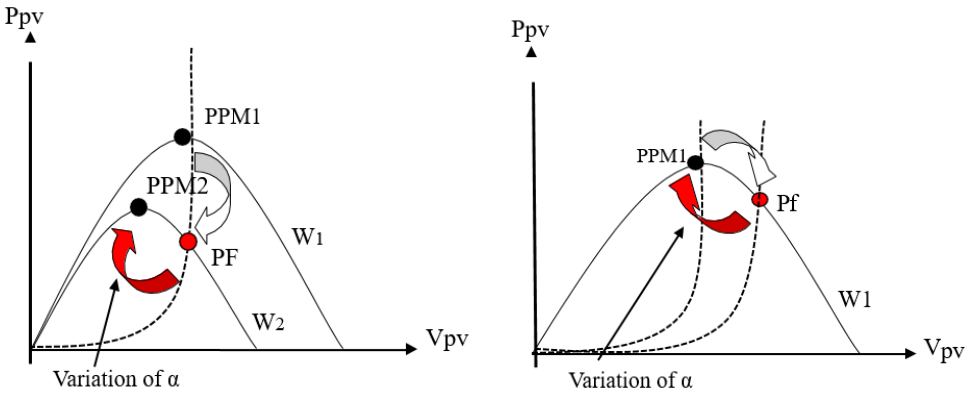

(a) fluactuation1 (b) fluactuation2

Figure 2.6: Fluctuation of the PPM with the intensity of illumination

2.4.2 Different types of MPPTs algorithms

The MPPT controller adjusts the operating conditions of the panel, such as voltage and current, to ensure that the system operates at its highest possible efficiency.

While there are no specific "commands" for MPPT, MPPT controllers typically utilize control algorithms to continuously monitor the output power of the solar panel and make adjustments accordingly. These adjustments are based on the voltage and current measurements to track the maximum power point.

The MPPT controller can be programmed or configured with parameters that determine its behavior and performance. These parameters may include:

- Step size: It defines the increment or decrement in voltage or current during the tracking process.
- Tracking speed: It determines how quickly the MPPT controller responds to changes in irradiation or temperature to track the maximum power point.
- Voltage and current limits: The MPPT controller may have configurable limits to ensure the system operates within safe operating conditions.
- Sampling rate: It defines how frequently the controller samples the voltage and current values to calculate the power output and adjust the operating conditions.
- Control mode: MPPT controllers may offer different control modes, there are various examples of MPPT technologies like The $Hill - Climbing$, IncCond and Perturbe & Observe techniques and they are the most widely used because of their simplicity. The operating principle of these three techniques is briefly summarized below.

2.4.3 MPPT algorithm classification

MPPT algorithms can be categorized as conventional, soft computing, or hybrid methods. This classification can have sub-categories like standard or improved algorithms, online or offline operation, and based on the working background. 2.7shows a general classification of MPPT algorithms.

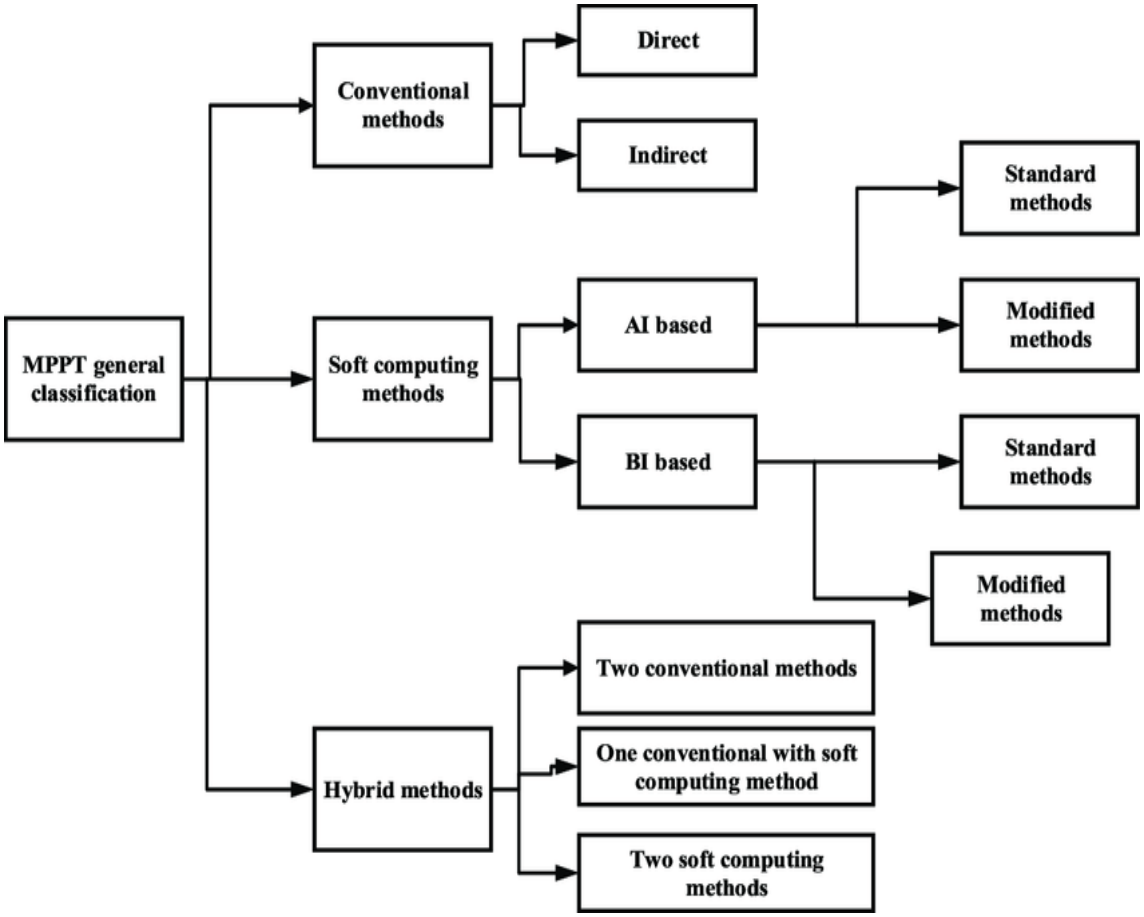

Figure 2.7: General MPPT methods classification

2.4.4 MPPT Algorithms

The principle of these MPPT commands is to find the MPP by keeping a good fit between the MPP and the load to ensure the transfer of maximum available electrical power[18].

In this chapter, there are various examples of MPPT technologies that serve to improve.

The HC, INC, and $P\&O$ techniques are the most widely used because of their simplicity and ease of implementation. The operating principle of these three techniques is briefly summarized below:

Perturb and Observe (P&O) Algorithm

The perturbation and observation method, commonly known as the 'P&O' method, is widely utilized in the industrial due to its simplicity in implementation. This algorithm

works by perturbing the system, specifically by increasing or decreasing the operating voltage of the PV module, and observing the corresponding effect on the output power of the PV array[19].

The flow chart that explains perturb and observe algorithm visually are shown in figure 2.8.

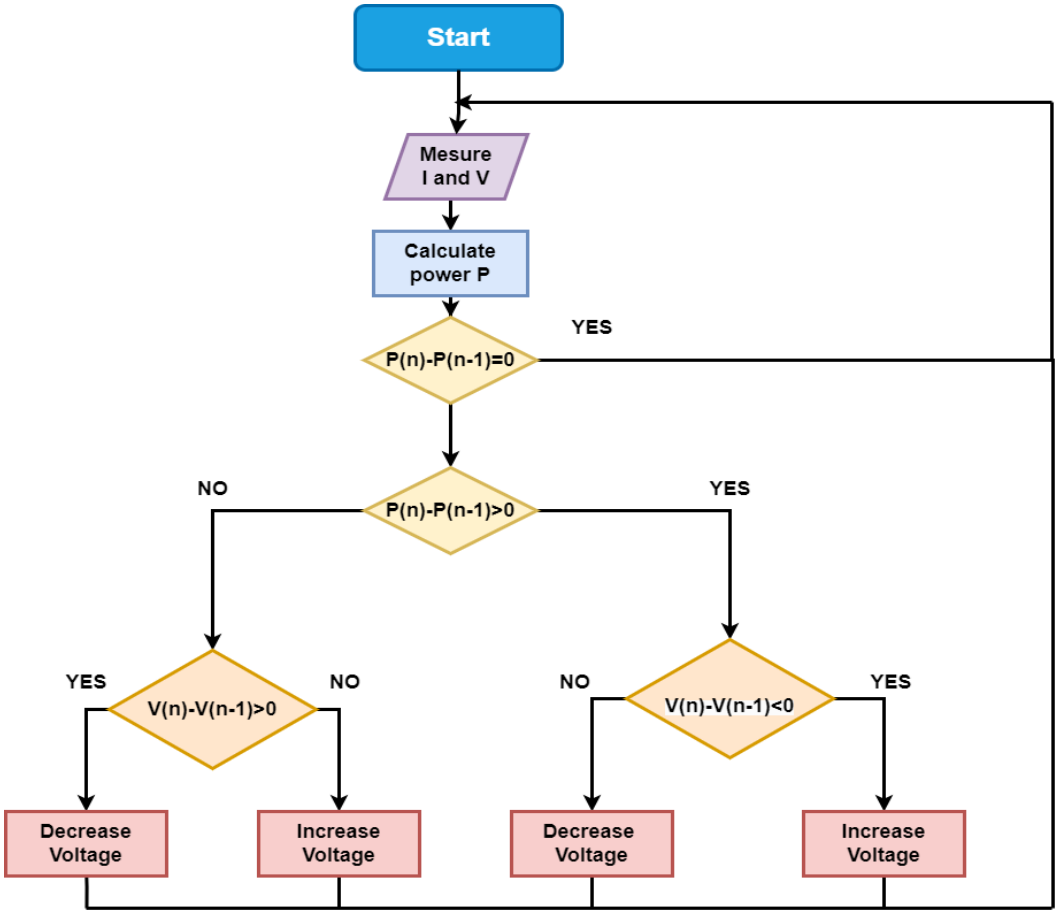

Figure 2.8: P&O algorithm flowchart

The principle of P&O type MPPT controls (figure 2.9) consists in disturbing the photovoltaic panel voltage Vpv with a low amplitude around its initial value and analyzing the behavior of the resulting power variation P_{pv}. Thus, as illustrated in the figure 13, it can be deduced that if a positive incrementation of the voltage V_{pv} generates an increase in the power P_{pv}, this means that the operating point is to the left of the PPM. If, on the contrary, the power decreases, this implies that the system has exceeded the PPM. A similar reasoning can be made when the voltage decreases. From

these various analyzes on the consequences of a voltage variation on the characteristic $P_{pv}(V_{pv})$, it is then easy to locate the operating point with respect to the PPM, and to make the latter converge towards the maximum power through an appropriate control order [20].

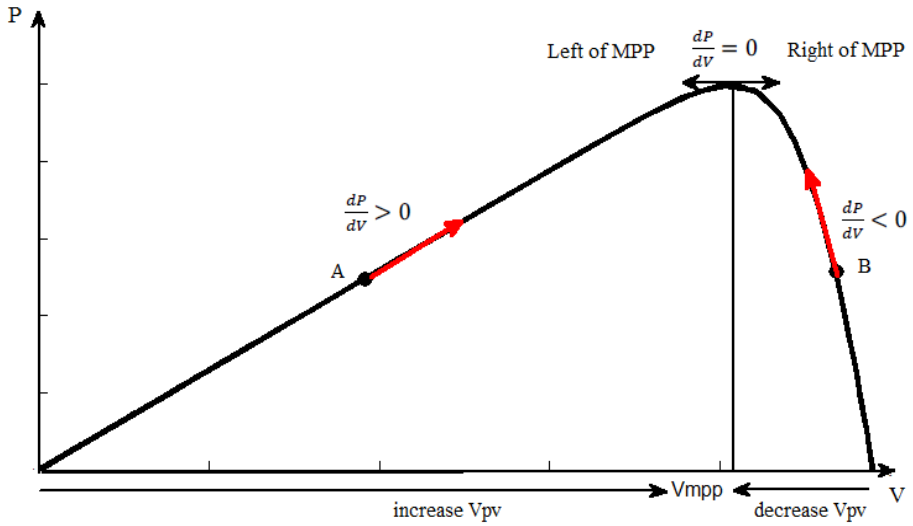

Figure 2.9: Principle of operation of the MPPT P&O

Incremental Conductance (INC) Algorithm

The Incremental Conductance (INC) method was developed based on observations of the P-V characteristic curve. It was designed as an alternative to the Perturb and Observe (P&O) method, aiming to address some of its limitations. The INC method aims to improve tracking speed and enhance energy production in environments with significant changes in irradiation levels [21]. It determines the Maximum Power Point (MPP) by analyzing the relationship between the derivative of current with respect to voltage (dI/dV) and the negative ratio of current to voltage ($-I/V$).

In the INC method, if the derivative of power with respect to voltage (dP/dV) is negative, it indicates that the MPP lies to the right of the current operating point. Conversely, if the MPP is positive, the INC method adjusts the operating point towards the left [22].

The equation of INC method is :

$$\begin{aligned} \frac{dP}{dV} &= \frac{d(V.I)}{dV} = I\frac{dV}{dV} + V\frac{dI}{dV} \\ &= I + V\frac{dI}{dV} \end{aligned} \tag{2.24}$$

MPP is reached when $dP/dV = 0$ and:

$$\frac{dI}{dV} = -\frac{I}{V} \tag{2.25}$$

so:

$$\begin{cases} \frac{dP}{dV} > 0 \text{ then } V_{\mathrm{p}} < \mathrm{V_{mpp}} \\ \frac{dP}{dV} = 0 \text{ then } \mathrm{V_p} = \mathrm{V_{mpp}} \\ \frac{dP}{dV} < 0 \text{ then } V_{\mathrm{p}} > \mathrm{V_{mpp}} \end{cases} \tag{2.26}$$

If the Maximum Power Point (MPP) is on the right side, it means that the rate of change of current with respect to voltage (dI/dV) is smaller than the negative ratio of current to voltage (-I/V). In this case, the photovoltaic (PV) voltage needs to be decreased to reach the MPP. The Incremental Conductance (INC) method is used to find the MPP, improve PV efficiency, reduce power loss, and lower system costs. INC algorithm can be seen on Figure 2.10.

Hill-Climbing Algorithm

The Hill Climbing control technique aims to find the maximum power point of a generator by adjusting its operating point along the characteristic curve. The technique considers two possible slopes and continues the adjustment until the maximum power point is reached. Mathematically, this occurs when the derivative of the photovoltaic power with respect to the operating point dP_{pv}/dD is forced to zero by the control command (Figure 2.11) [23]. In simpler terms, the Hill Climbing method fine-tunes the generator's operating point to maximize its power output.

2.5 Linear and non-linear controllers for MPPT

The regulator represents the intelligent element of a system, it is added outside the system to be controlled, and it makes it possible to improve the performance of the

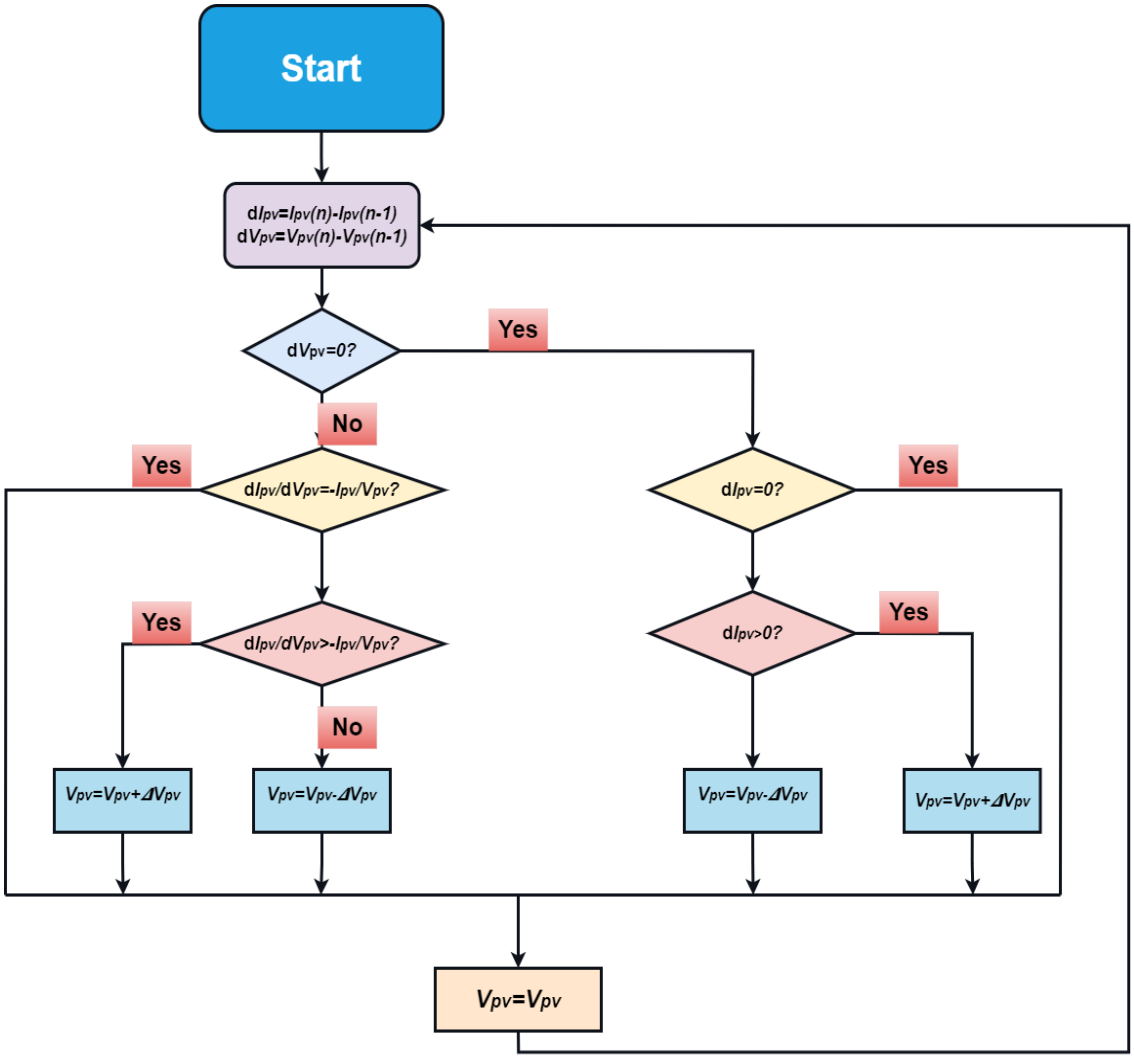

Figure 2.10: INC algorithm flowchart

system that it controls whether transient or permanent.

To enhance the regulation of our photovoltaic (PV) system, we have chosen to employ both a PI regulator (Proportional-Integral regulator) and the non-linear Integral sliding mode control $ISMC$ which is our objective in this thesis. This decision is driven by our aim to improve the accuracy of the control loop and achieve reduce static error.

The PI regulator consists of two integral components: proportional control and integral control. The Proportional control responds to the immediate error between the desired Set-point and the actual output, generating an output signal that is proportional to this error. This proportional term enables a swift response and helps minimize steady-state error.

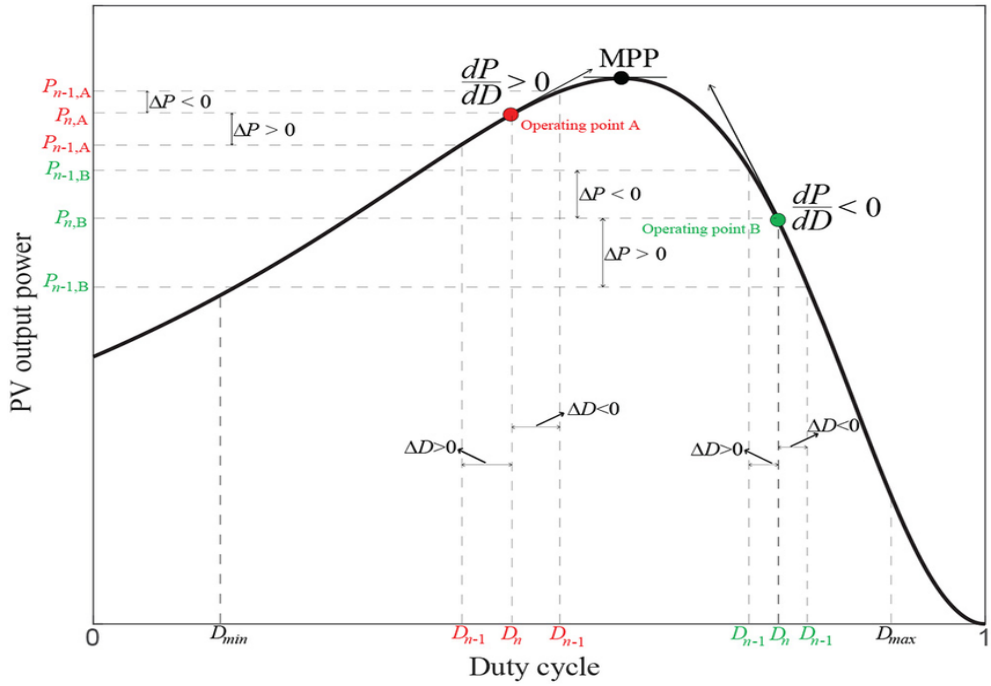

Figure 2.11: The relationship between PV power and the duty cycle of the MPPT boost converter

The integral control component of the PI regulator integrates past errors over time and adds this cumulative term to the proportional control output. By doing so, it effectively addresses any remaining steady-state error, gradually reducing it and enabling the system to reach and maintain the desired Set-point with greater accuracy.

In addition to the PI regulator, we have incorporated integral sliding mode control into our system.

Integral Sliding mode control is a robust control technique that enhances accuracy, particularly in the presence of disturbances or uncertainties. It involves the creation of a sliding.

2.5.1 PI controller

PI control is widely used in industry and is a common control structure in many control architectures, often incorporating proportional and integral actions. It is estimated that PI control is utilized in more than 90% of control systems [24].

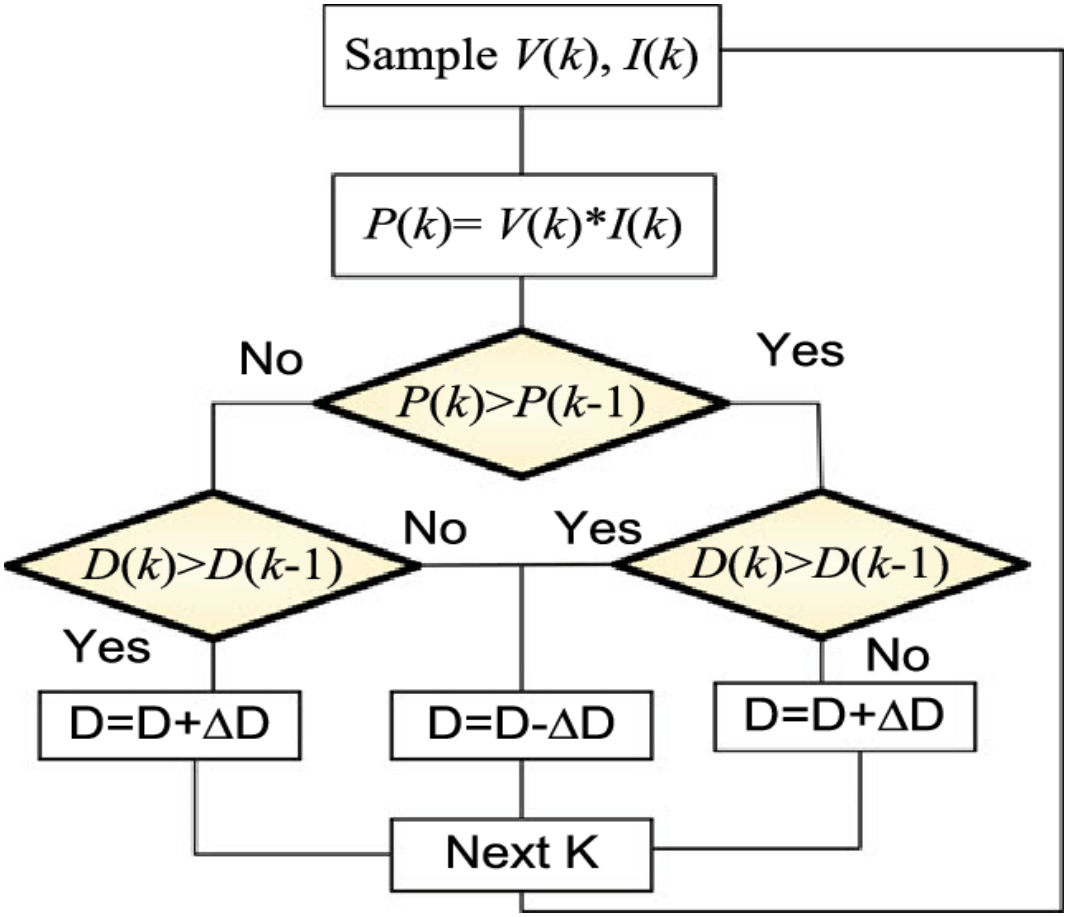

Figure 2.12: The flowchart of the HC-MPPT method

The principle of PI is based on the fact of delivering a control signal e(t) from the difference between the set-point r(t) and the measurement y(t), hence:

$$e(t) = r(t) - y(t) \tag{2.27}$$

In order to minimize e(t) three contributions are added to the output of the controller. Figure (III.4) presents the main structure of the PID [25].

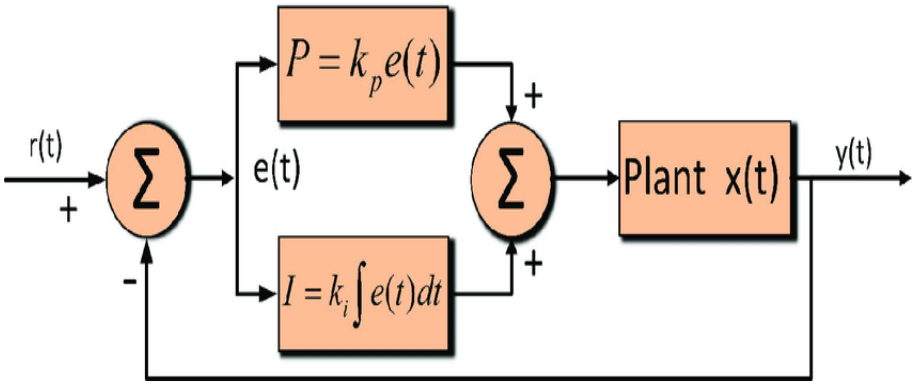

Figure 2.13: Block diagram of a PID controller

The output u(t) of the PI can therefore be calculated as follows :

$$\mathrm{u(t)} = \mathrm{k_p} + \mathrm{k_i} \int_0^{\tau} e(t)\mathrm{dt} \tag{2.28}$$

with:

K_p: is the proportional coefficient.

K_i : is the integral coefficient.

The adjustment of a Proportional-Integral (PI) regulator involves various methods. These methods include trial-and-error, Ziegler-Nichols, Cohen-Coon, frequency response analysis, and model-based optimization techniques. $MEPLAT$, an example of a model-based optimization technique, can be employed to fine-tune the PI. controller parameters. By utilizing mathematical models and optimization algorithms, $MEPLAT$ aids in achieving optimal control performance in PI. regulation.

2.5.2 Integral sliding mode control $ISMC$

Integral Sliding mode control ($ISMC$) is a nonlinear control technique featuring remarkable properties of accuracy, robustness, and easy tuning and implementation. The fundamental concept behind sliding regime control is to initially attract the system states towards a carefully selected region. Once the states are within this region, the next step is to devise a control law that ensures the system remains within it consistently. In other words, sliding regime control involves the sequential tasks of

attracting the states to the chosen region and subsequently determining a control law that guarantees the system's continuous presence within that region. The control by sliding mode generally comprises two terms as shown hereafter [26, 27] :

$$u = u_{eq} + u_{dis} \tag{2.29}$$

With:

- U_{eq}: A continuous term, called equivalent command.
- U_{dis}: And a discontinuous term, called switching control.

The equivalent command

Utkin's proposed method involves considering an equivalent command in sliding mode control. This command simulates the system's behavior as if it were controlled by an ideal sliding regime. In this regime, the operating point remains on the desired sliding surface, and the derivative of the area function, denoted as $\dot{S}$, remains zero ($\dot{S}$= 0).

The switching command

The switching command is utilized to enforce the requirement that the system's operating point remains close to the desired sliding surface. Its primary objective is to validate the conditions of attractiveness. By imposing this command, the system is effectively guided to maintain proximity to the sliding surface, thereby ensuring stability and the desired behavior within the sliding mode control framework.

$$U_{dis} = -K.\,\mathrm{sign}(S) \tag{2.30}$$

The gain K is chosen to guarantee stability, speed and to overcome external disturbances can affect the system.

The sign "$\cdot$" indicates the recall of the operating point to the surface at any instant of functioning.

The function sign(s)is defined by:

$$\text{Sign}(S) = \begin{cases} +1 & \text{Si} \quad S > 0 \\ -1 & \text{Si} \quad S < 0 \end{cases} \tag{2.31}$$

The structure of a sliding mode controller comprises two essential components: a linearizing part referred to as U_{eq}, and a stabilizing part denoted as U_{dis}, The linearizing part aims to transform the system dynamics into a linear form, while the stabilizing part is responsible for ensuring system stability by driving it toward the sliding surface and maintaining it within that surface..

2.5.3 The ISMC flowchart

The ISMC flowchart shown on Figure 2.14

2.5.4 Integral sliding mode controller design for MPPT application

We consider the dynamic boost converter equation as follows :

$$\begin{cases} \dot{x}_1 = \frac{-(1-u)}{L} x_2 + \frac{V_{pv}}{L} \\ \dot{x}_2 = \frac{(1-u)}{C} x_1 - \frac{x_2}{RC} \end{cases} \tag{2.32}$$

with:

$$\dot{x}_1 = \frac{di}{dt}, \dot{x}_2 = \frac{dv_o}{dt} \tag{2.33}$$

Using integral sliding mode control ($ISMC$), the sliding manifold can be defined as follows:

$$S = e + K \cdot \int edt \tag{2.34}$$

Where the error between the output voltage (V_O) and the reference voltage (V_{ref}) is writing as follow :

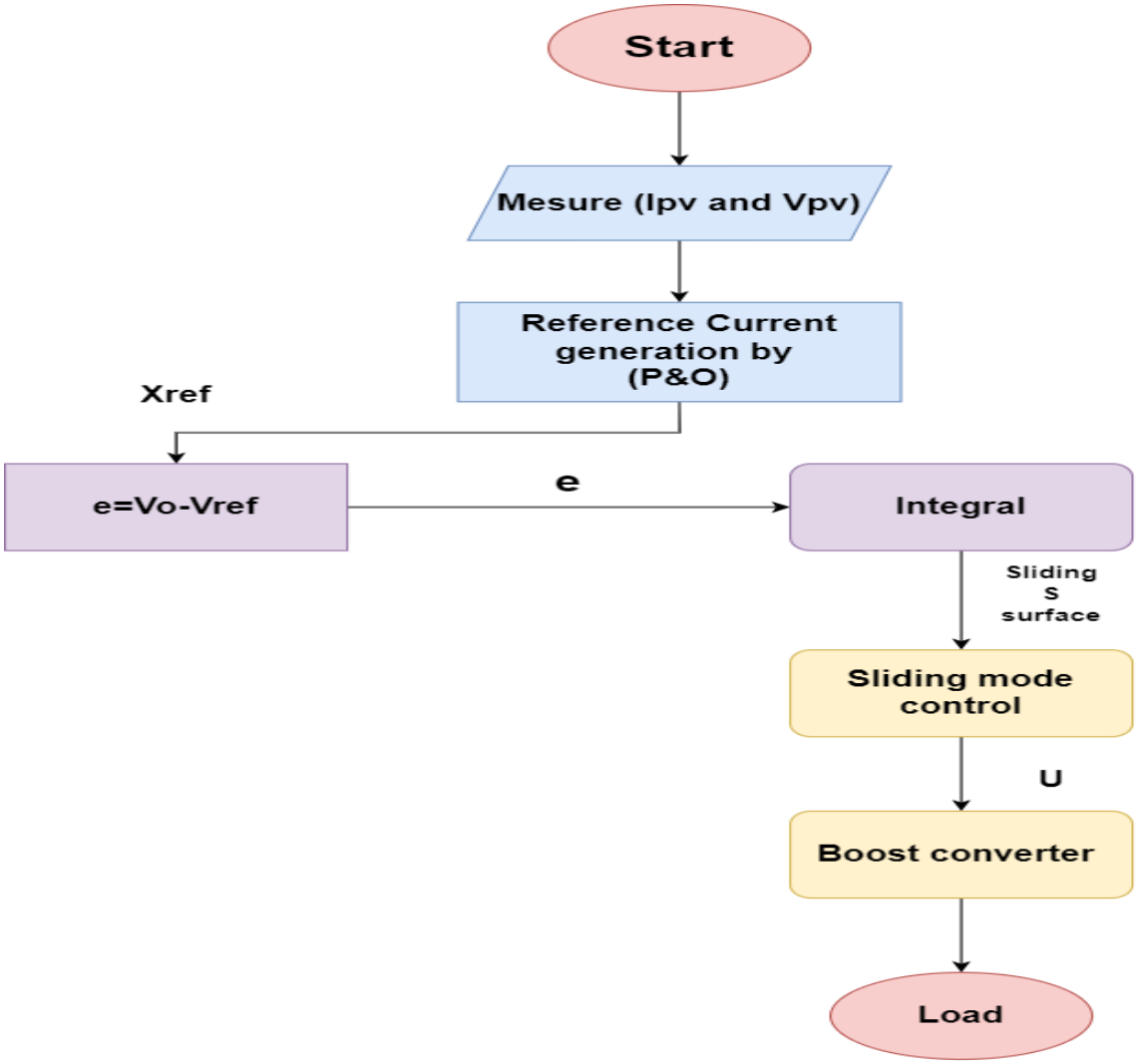

Figure 2.14: ISMC flowchart

$$e = Vo - Vref \tag{2.35}$$

The derivations of equation ((2.35)) give leads to :

$$\dot{e} = \dot{Vo} - \text{ Vref} \tag{2.36}$$

The main objective of our approach is to ensure that the sliding surface reaches a value of zero. Consequently, by differentiating the sliding surface, we obtain the following results:

$$\dot{S} = \dot{e} + K_s e = \dot{V}_{\text{ref}} - \dot{V}_{\text{o}} + K_s \left(V_{\text{ref}} - V_o\right) \tag{2.37}$$

Because $\dot{S} = 0$ and by using Eq ((2.35)) one can write the equivalent control of sliding mode as :

$$\dot{V}_{ref} - \left(\frac{(1-u)}{C} i - \frac{V_o}{RC}\right) + K_s e = 0 \tag{2.38}$$

So:

$$\dot{V}_{ref} + K_s e = \left(\frac{(1-u)}{C} i - \frac{V_o}{RC}\right) \tag{2.39}$$

then:

$$\dot{V}_{\text{ref}} + K_s e + \frac{V_o}{RC} = \frac{(1-u)}{C} i \tag{2.40}$$

and:

$$1 - u = \left(\dot{V}_{\text{ref}} + K_s e + \frac{V_o}{RC}\right) \frac{C}{i} \tag{2.41}$$

Finally:

$$U_{eq} = 1 - \left(\dot{V}_{\text{ref}} + K_s e + \frac{V_o}{RC}\right) \frac{C}{i} \tag{2.42}$$

The output signal control of integral sliding mode control is given by:

$$u = u_{eq} + u_{dis} \tag{2.43}$$

$$U = 1 - \left(\dot{V}_{ref} + K_s e + \frac{V_o}{RC}\right) \frac{C}{i} - K \,\text{sign}(S) \tag{2.44}$$

System stability prove

To demonstrate the stability of the system in the context of sliding regime control, the Lyapunov criteria are utilized. In this application, a specific Lyapunov function candidate is chosen:

$$V = \frac{1}{2}S^2 \tag{2.45}$$

The derivation time of Eq(2.45) give as :

$$\dot{V} = S \cdot \dot{S} \tag{2.46}$$

the stability is guaranteed, if the Lyapunov function derivative Eq(2.46) is always negative. By replacing Eqs(2.37) and (2.34) in Eq(2.46), one can obtain:

$$\dot{V} = \left(e + K \cdot \int edt\right)\left(\dot{V}_{ref} - \frac{(1-u)}{C}i - \frac{V_o}{RC}\right) + K_s e \tag{2.47}$$

By replacing Eq(2.44)in Eq(2.47)

$$\dot{V} = \left(\frac{-C}{i}\left(K_s e + \dot{V}_{ref} + \frac{V_o}{RC}\right) + 1\right) - K\,\mathrm{Sign}(S) \tag{2.48}$$

also By replacing Eq(2.43) in Eq(2.48)

$$\dot{V} = S\left(\dot{V}_{ref} - \frac{i}{c} - 1\left(K_s e + \dot{V}_{ref} + \frac{V_o}{RC}\right) + \frac{i}{c}\right) - \frac{i}{C}K\,\mathrm{Sign}(S) - \frac{V_o}{RC} + K_s e \tag{2.49}$$

Simplifying the last equation we obtain:

$$\dot{V} = S\left(-2\frac{V_o}{RC} - \frac{i}{C}K\,\mathrm{sign}(S)\right) < 0 \tag{2.50}$$

Where k is a positive value. this last equation is always negative which proves that the system is stable

2.6 Conclusion

In this chapter, we explored the integration of $MPPT$ algorithms, DC-DC converters, and PI/Sliding Mode regulators in photovoltaic (PV) systems. $MPPT$ algorithms, such as P&O, $IncCond$, and Hill-Climbing, enable efficient power extraction by tracking the maximum power point of solar panels.

The selection of the appropriate algorithm depends on specific performance requirements and implementation complexity.

DC-DC converters play a vital role in voltage conversion and power optimization, with Boost, typologies being commonly used. The inclusion of PI and Sliding Mode regulators enhances control accuracy and stability, with PI controllers offering simplicity and Sliding Mode control providing robustness against uncertainties. Comparative analysis assists in identifying the optimal combination for achieving high tracking efficiency and system performance.

Chapter 3

Simulation Results

3.1 Introduction

Solar energy is considered a secure and reliable energy source. However, the amount of electricity generated by photovoltaic (PV) panels can be influenced by various factors including dust, temperature, cloud cover, geographical location, and the intensity of solar radiation. In the previous chapter, we established mathematical models for the PV system and boost converter. In this chapter, our goal is to analyze and compare different algorithms—namely, classical algorithms such as P&O, IC, and HC, as well as a linear controller (PI) and a nonlinear controller (ISMC). The purpose is to determine the most effective method for locating and tracking the Maximum Power Point (MPP) of the PV system. These algorithms have been designed as controllers to provide the boost converter with the optimal duty cycle required to achieve the MPP.

3.2 PV system and boost characteristics

3.2.1 PV System

A PV system combines PV panel, Dc-Dc converter, $MPPT$ controller, and load as shown in Figure 3.1. The $MPPT$ controller takes PV panel voltage and current values as input, performs necessary computations and generates the required gate pulse for

the switching element in the converter, such that the impedance mismatch between source and load can be minimized.

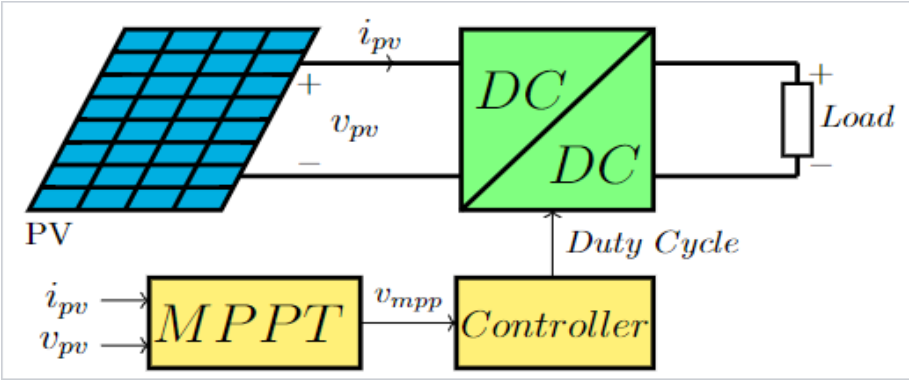

Figure 3.1: Block diagram of PV system

3.2.2 PV characteristic used

PV panel is a group of PV cells connected together forms a PV panel .In order to get high output voltage, PV cells are connected in series and parallel connected PV cells yield high output current.

In this work, highly efficient multi-crystal $KyoceraKC200GT$ solar panels are used in this simulation. Figure 3.2 shows I-V and P-V characteristics of the PV panel at 25 °C temperature and at decrement irradiance.

Figure 3.3 depicts P-V and I-V characteristics at constant irradiance of 1000 W/m2 and decrement temperatures.

3.2.3 DC-DC converters

Figure 3.4 shows the Boost power converter that is used to steps up the input voltage magnitude to a required output voltage magnitude without the use of a transformer.

The basic components of a boost converter are an inductor, a capacitor, a diode and a high-frequency switch as illustrated .

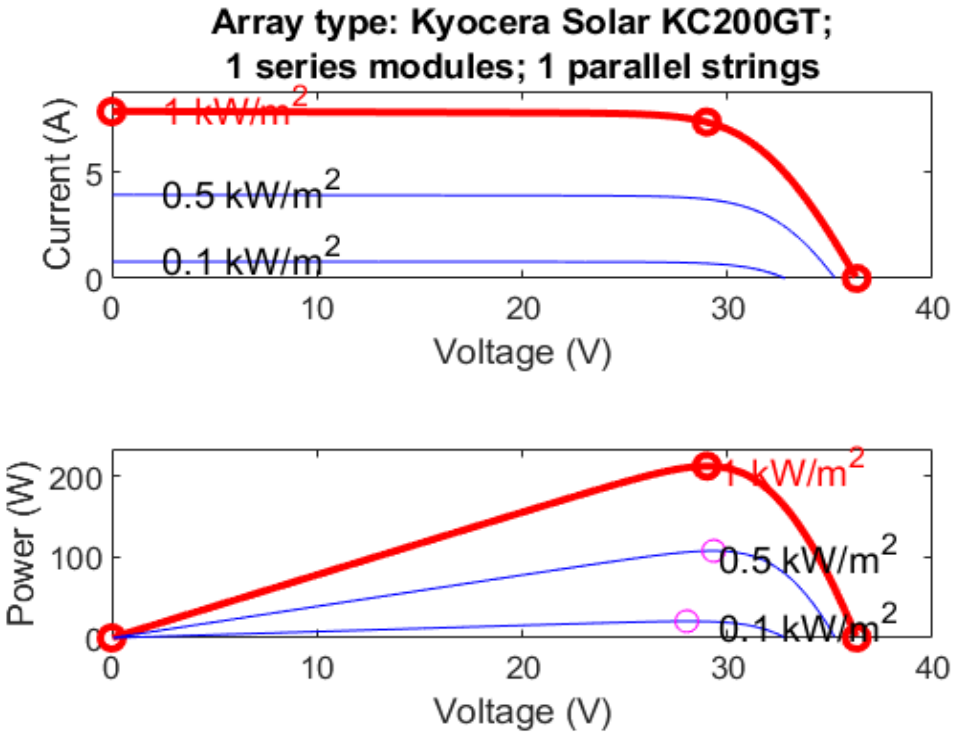

Figure 3.2: I-V and P-V characteristics of the PV panel at 25 °C temperature and at decrement irradiance.

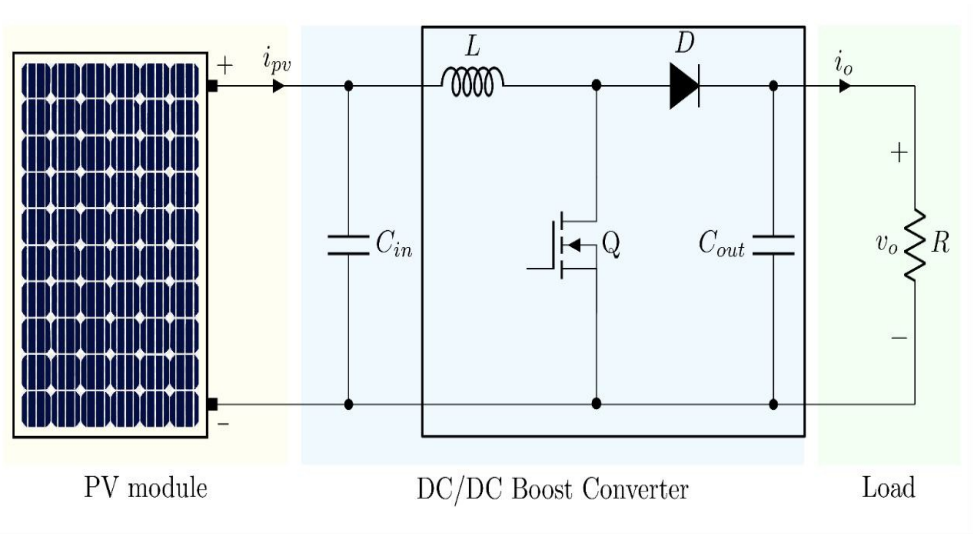

Figure 3.4: *PV* system with the boost converter

The *PV* panel parameters under standard test conditions (*STC*) and the specifications for the boost converter are presented in table 3.1

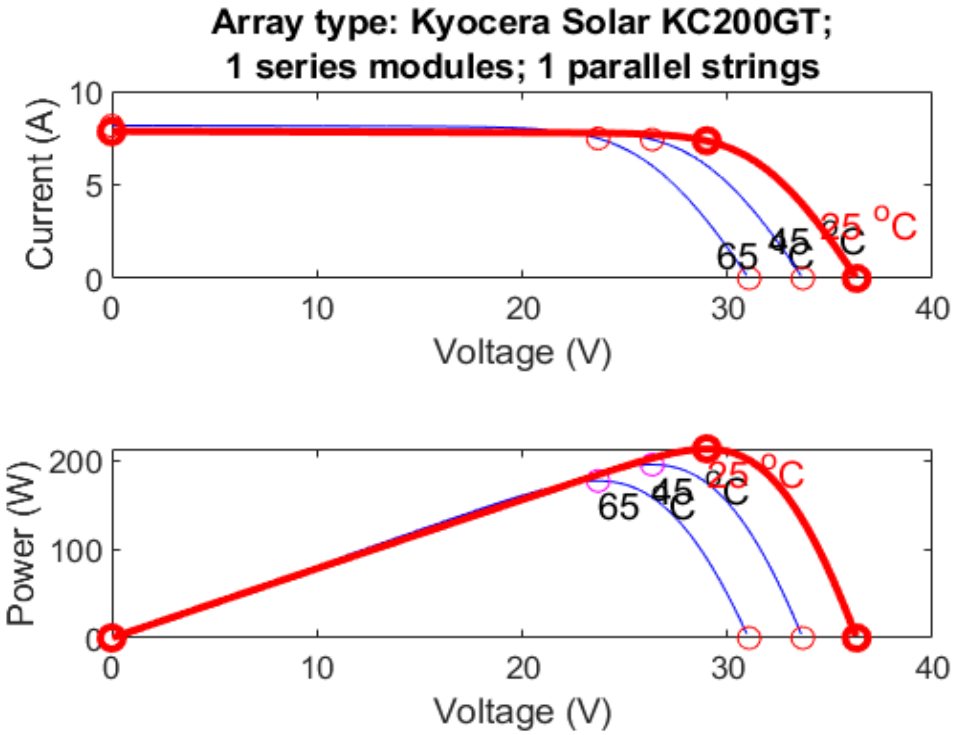

Figure 3.3: I-V and P-V characteristics at constant irradiance of 1000W/m2 band decrement temperatures.

PVmodule characteristics		**PVplant parameters**		**DC-DCboost converter**	
Nc	**60**	**Np**	**1**	**fs(kHz)**	**20**
VOC(V)	**36.3**	**Ns**	**1**	**L(H)**	**0.0061**
ISC(A)	**7.84**	**N**	**1**	**Cin(uF)**	**1.2606**
VMPP(V)	**29**	**PT(kW)**	**213.15**	**Cout(uF)**	**139.68**
IMPP(A)	**7.35**	**Load value $R(\Omega)$**	**20**	- -	
PMPP(W)	**213.15**	**Simulation step time(µs)**	**1**	- -	

Table 3.1: The PV panel parameters and the boost converter

3.2.4 PI Controller

The *PI* controller is formulated in Eq 3.1

$$\mathrm{u(t)} = \mathrm{k_p} + \mathrm{k_i} \int_0^{\tau} e(t)\mathrm{dt} \tag{3.1}$$

Where kp is the proportional gain, ki is the integral gain. The parameters of PI that are used in the three algorithms have been calculated by using the turning function in Matlab and are presented in table 3.2.

PI	
Kp	Ki
3	1

Table 3.2: The parameters of PI

3.3 Simulation analysis results and discussion

In this simulation, a comparative study is conducted to analyze the performance of three Maximum Power Point Tracking (MPPT) algorithms: the Hill Climbing algorithm, the Perturb and Observe (P&O) algorithm, the Incremental Conductance (INC) algorithm, PI controller and ISMC controller. These algorithms are applied to a DC/DC Boost converter in order to assess their effectiveness. The PV panel is connected to the boost converter, as illustrated in Figure 3.5. The objective of the designed PV system is to efficiently transfer electrical power from the PV array to the resistive loader. The simulation analysis and results are obtained using MATLAB/Simulink. The figures below present the obtained simulation results, considering a fixed temperature of 25°C and varying irradiation values as shown in Table 3.3.

Irradiances on the modules (W/m²)		
Cases	Applied time (s)	Irradiation
1	[0s <t<2s]	1000
2	[2s <t<3s]	800
3	[3s <t<4s]	600
4	[4s <t<5s]	800

Table 3.3: Irradiation values.

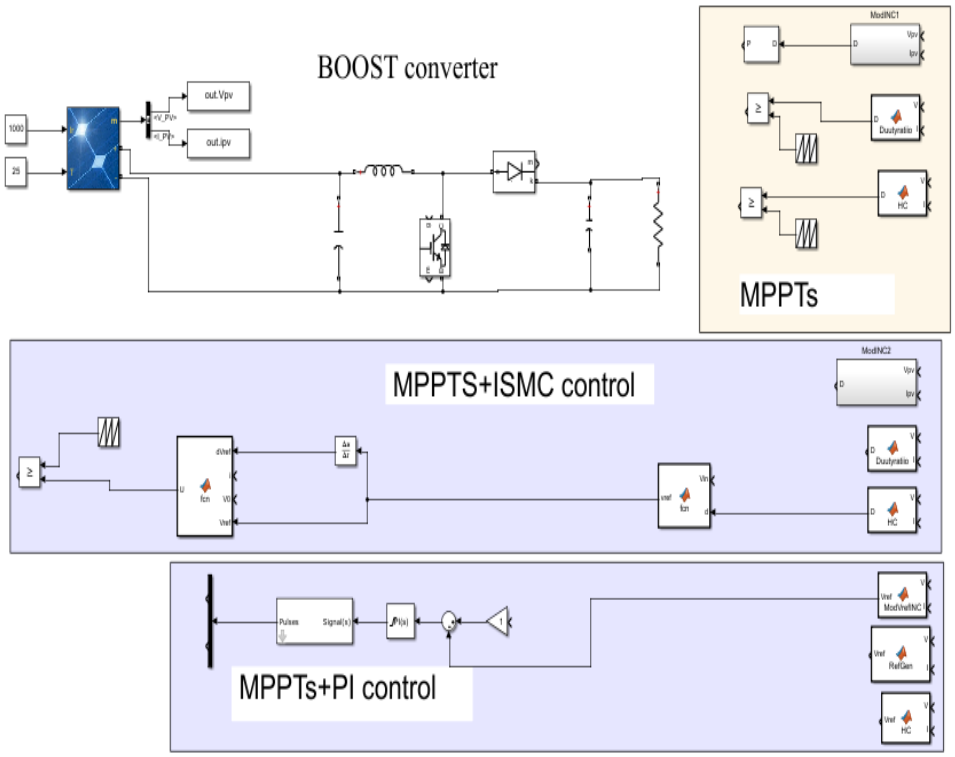

Figure 3.5: Detailed simulation circuit of PV system model

3.3.1 Evaluating the Effectiveness of Classical MPPT Algorithms: Results and Analysis

Figure 3.6 depicts the variation of irradiance over time, which is applied to the photovoltaic (PV) module. In the first case (Figure 3.6), the irradiance begins at $1000W/m^2$ until the second. In the first second, after that, the irradiance will be decreased from $1000W/m^2$ to $800W/m^2$ by one step-down of $200W/m^2$ until the third- second. In the third- second, step-down irradiance will be decreased from $800W/m^2$ to $600W/m^2$ until the fourth second by a step size of $200W/m^2$. In the fourth second, another step-up change from $600W/m^2$ to $800W/m^2$ also occurs by a step size of $200W/m^2$ until the fifth second.

The obtained simulation results from the use of three MPPTs algorithms (P&o , IC and HC) are presented in Figures 3.7 and 3.9 respectively, for a fixed of temperature ($25C^0$) and for different irradiation values From the different responses, one can remark that the maximum power is reached for different values of irradiations (see Figures 3.7 and 3.8)). In fact, the generated power to the load is equal practically to the maximum

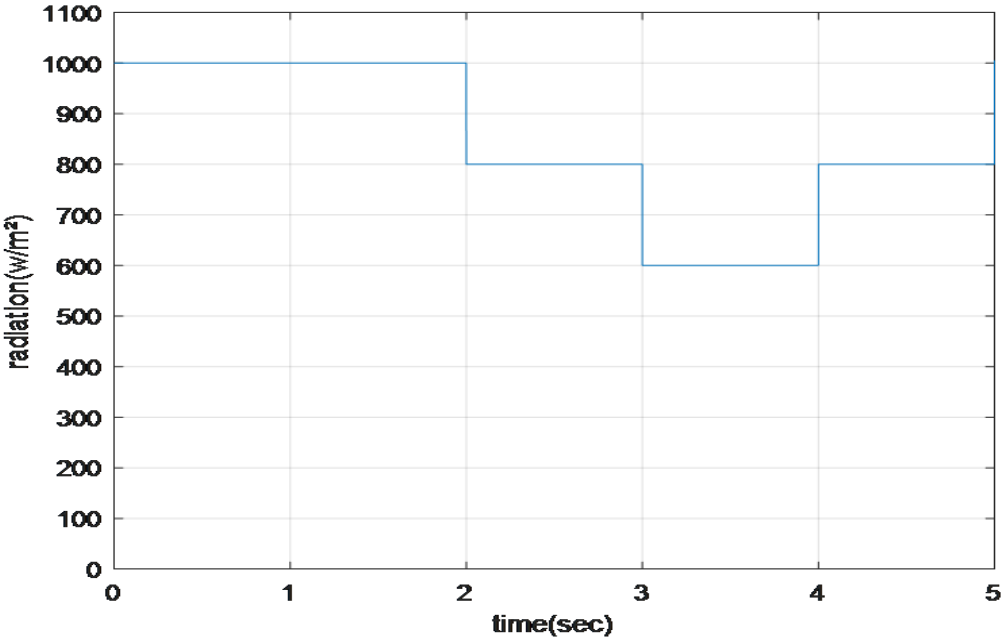

Figure 3.6: The irradiance scenario

power provided by the PV array with a little difference which is due to different system losses (see Figure 3.7(b) and Figure 3.8. By observing the system responses (Figure 3.4 and Figure 3.5) obtained by using the three techniques (IC, HC, and P&O), one can remark that:

- Analyzing the response profiles obtained using the Incremental Conductance (IC) technique, it is evident that the generated power corresponds to the changes in irradiation levels with a smooth transitional behavior. Notably, the IC technique demonstrates a favorable absence of power overshoot in the PV system, along with a fast settling time and minimized ripples in the produced power.
- The response profiles obtained from the utilization of the Perturb and Observe (P&O) and Hill Climbing (HC) algorithms indicate that these systems exhibit rapid changes in response with a favorable time response. However, it is worth noting that they also demonstrate higher ripples in the produced PV power, which may impact their overall stability.

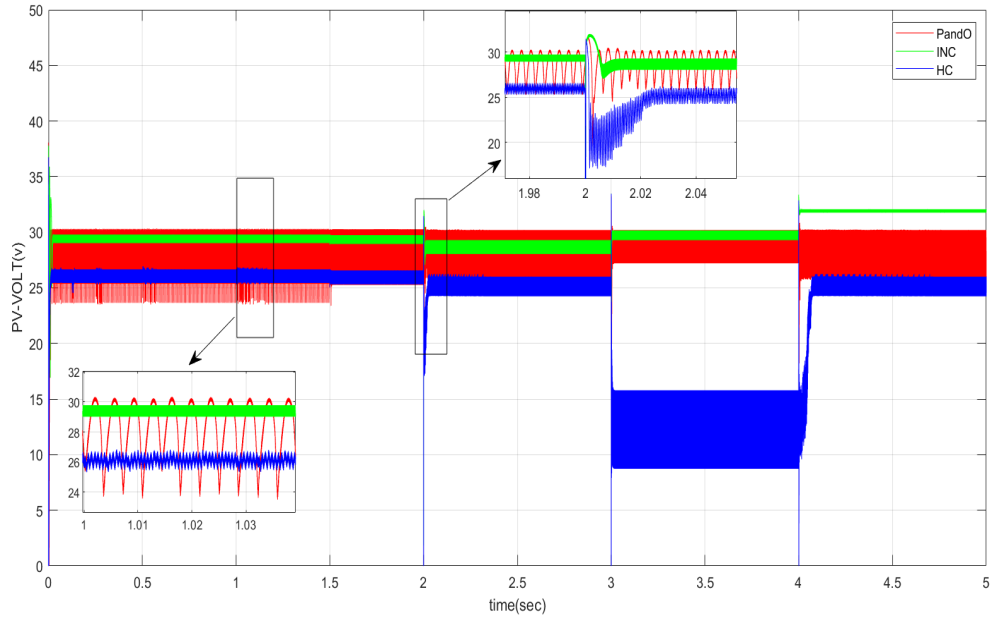

(a)

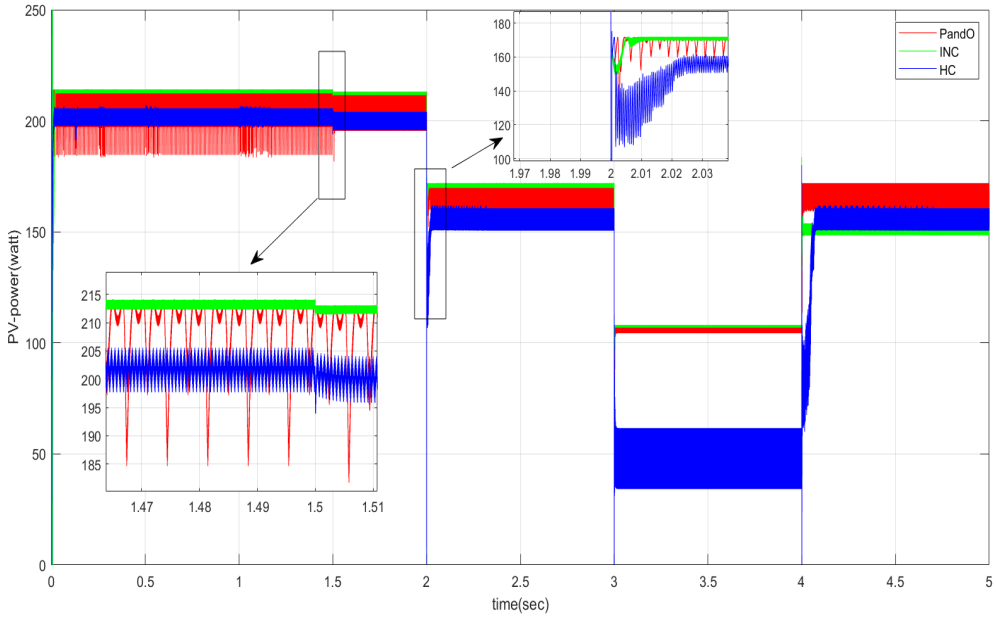

(b)

Figure 3.7: Simulation result of the panel with the three MPPTs technique, (a): PV voltage, (b): PV power.

Evaluating the effectiveness of nonlinear MPPT controller: results and analysis

The obtained simulation results from the use of the P&O in cascade with ISMC and P&O in cascade with PI are presented in Figures 3.10-3.13 respectively, for a fixed tem-

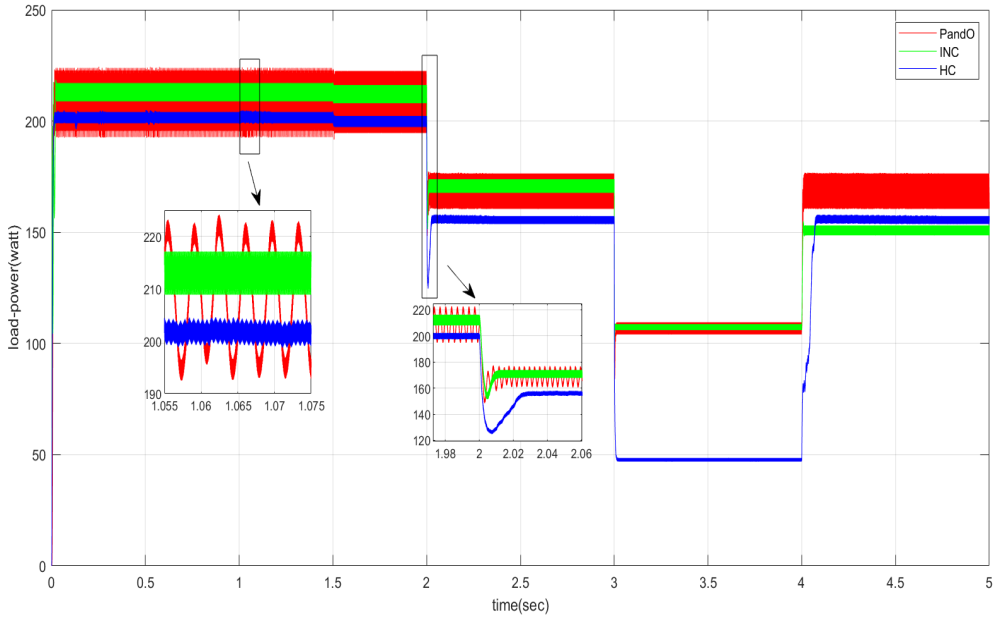

(a)

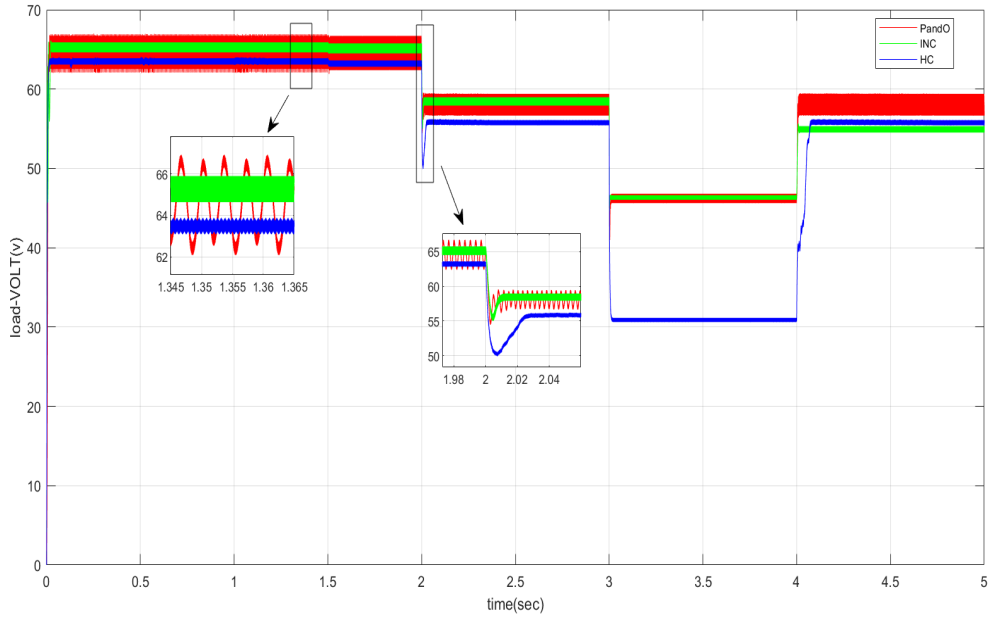

(b)

Figure 3.8: Simulation result of the boost output with the three MPPTs technique, (a): Power, (b): Voltage.

perature (250C) and for a different irradiation value ($1kW/m2$, $800W/m2$, $600W/m2$, $500kW/m2$ and $600W/m2$) (see Figure 3.9).

To compare the performances of ISMC and PI controllers, we examine the responses of PV voltages, PV power, and load power. Key factors for evaluating the effectiveness of the ISMC controller include state error and ripples. The simulation results are presented in Figures 3.10 to 3.13.

From these figures, it is evident that the ISMC controller exhibits superior dynamic performance when compared to the PI controllers. Additionally, the utilization of ISMC significantly reduces both ripples and state error. This improved performance can be attributed to the integral action and the nonlinear characteristics inherent to ISMC. The integral action effectively reduces state error and contributes to the overall enhanced performance of the controller.

.

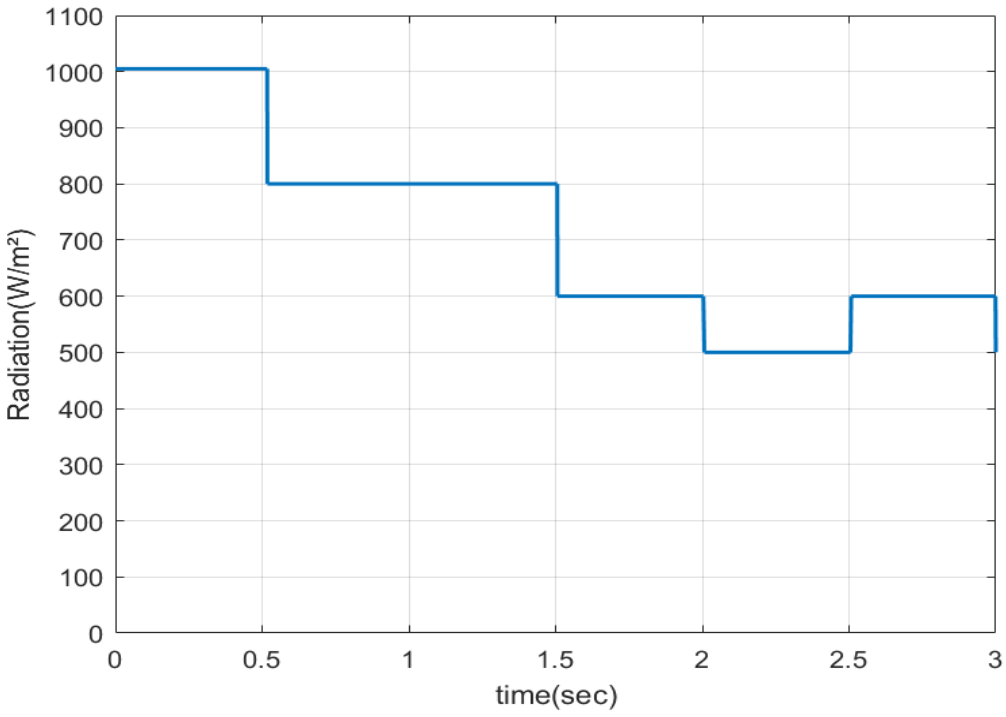

Figure 3.9: The irradiance scenario

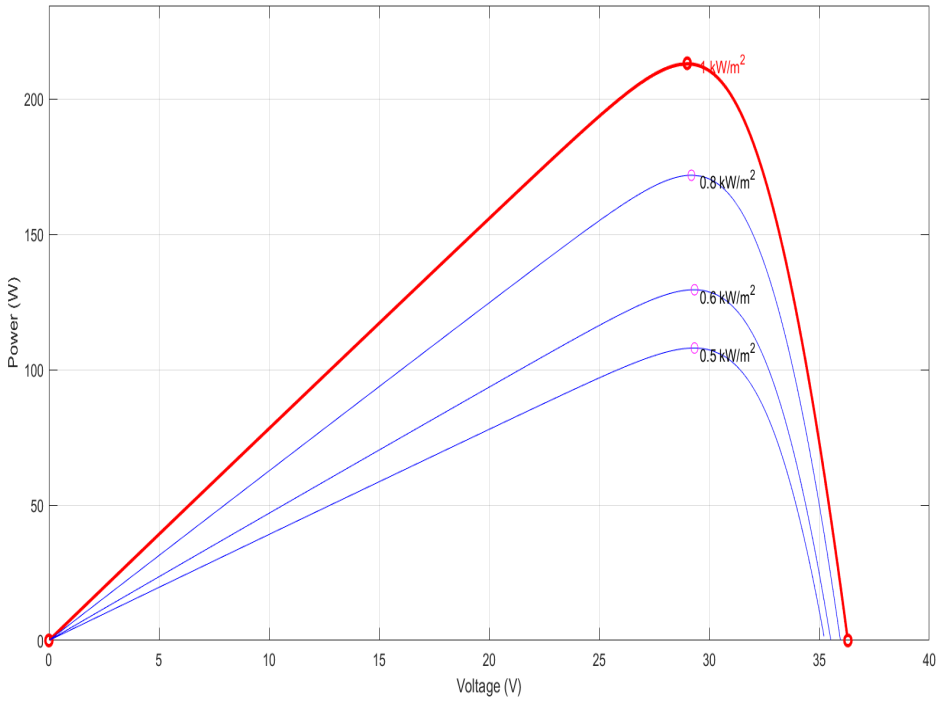

Figure 3.10: The Maximum Power Points

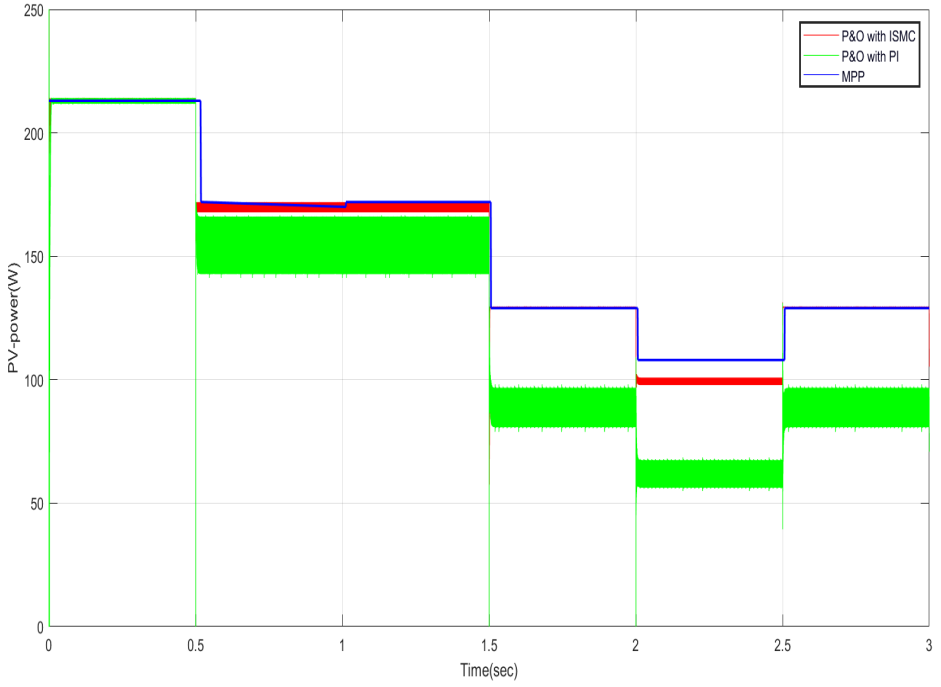

Figure 3.11: Simulation result of PV power of the P&O MPPT with PI and with ISMC

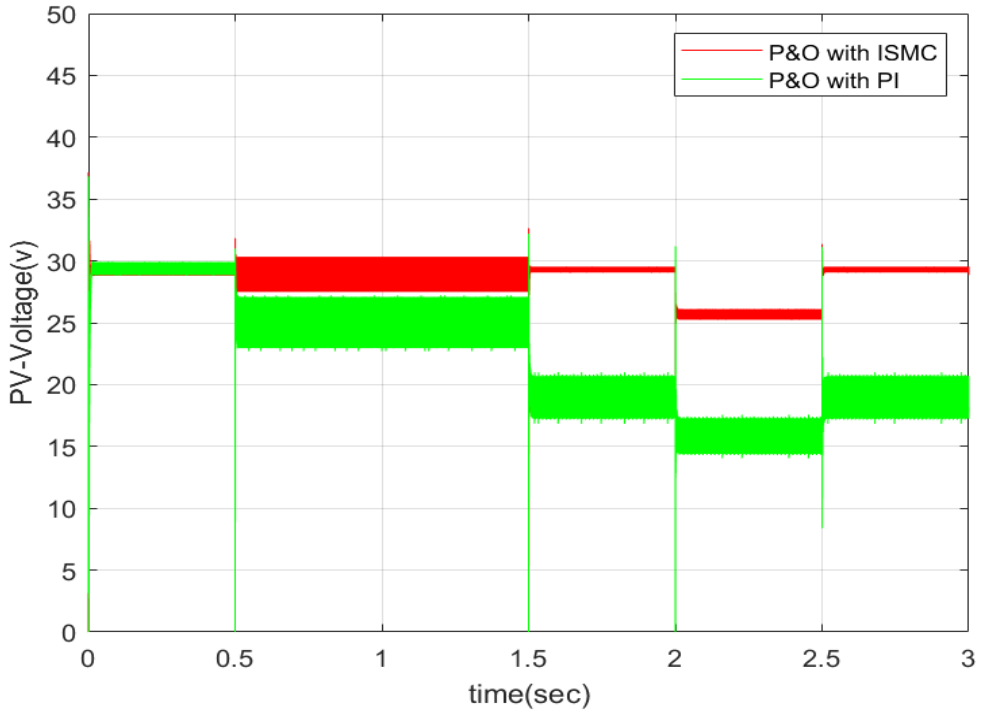

Figure 3.12: Simulation result of PV voltage of the P&O MPPT with PI and with ISMC

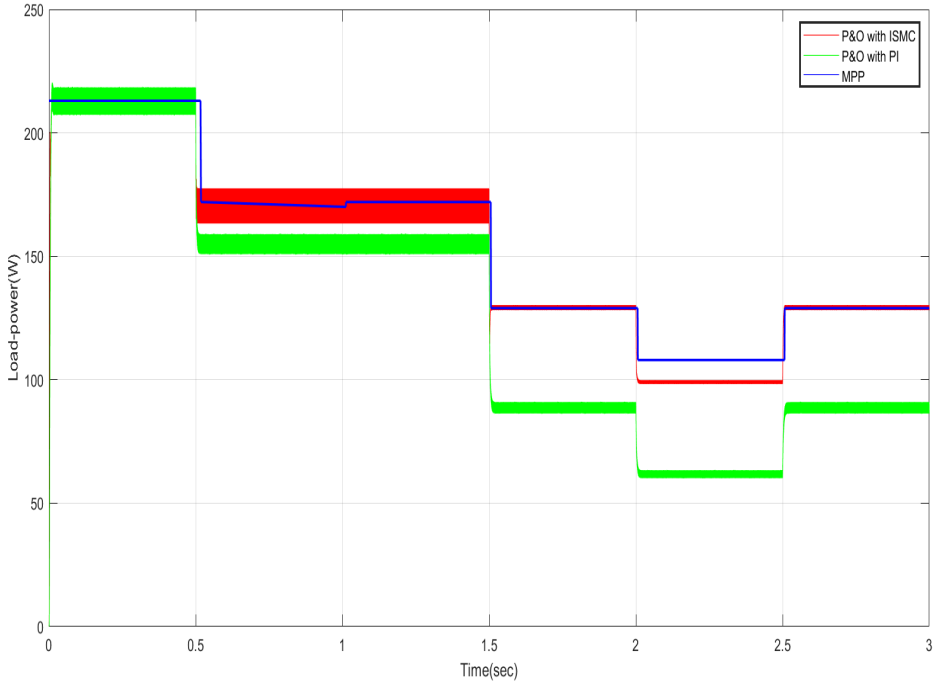

Figure 3.13: Simulation result of load power of the P&O MPPT with PI and with ISMC

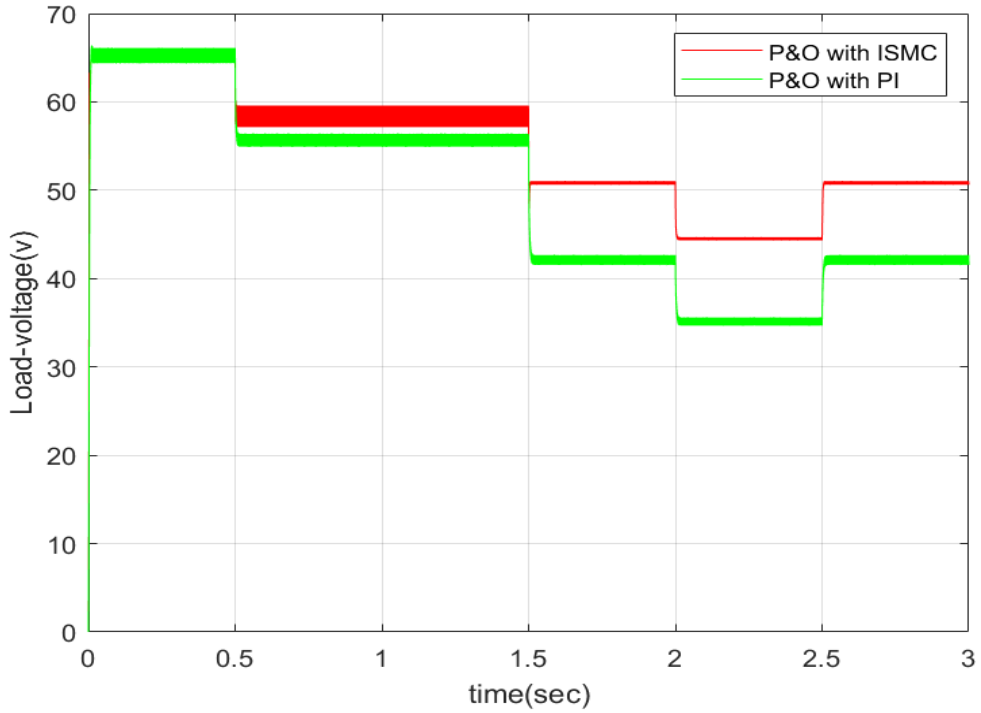

Figure 3.14: Simulation result of load voltage of the P&O MPPT with PI and with ISMC

3.4 Conclusion

In this chapter, our focus was on studying and comparing various classical MPPTs and two controllers in terms of their dynamic behavior. The selection of an appropriate algorithm depends on factors such as system complexity, environmental conditions, and desired performance. While the Hill Climbing algorithm is simple, it may encounter challenges with convergence and robustness. On the other hand, the P&O algorithm is easy to implement but can exhibit oscillatory behavior. Comparatively, the INC algorithm offers better accuracy and efficiency when compared to P&O. To choose the most suitable controller, it is crucial to consider the specific requirements of the DC/DC Boost converter and the operating conditions. Regarding the controller evaluation, the simulation assessed the performance of ISMC and PI controllers in combination with the P&O algorithm using various metrics, including tracking accuracy, dynamic response, efficiency, and stability. Furthermore, the ISMC accurately achieved the maximum power point, resulting in a suitable enhancement of system power quality.

Chapter 4

The experimental part

4.1 Introduction

To assess the outcomes of our experiments, we have implemented a distinct experimental setup. Specifically, we opted to evaluate the performance of the P&O algorithm with and without using the Integral Sliding Mode Control (ISMC). This approach allows us to determine the superiority of one controller over the other, while also verifying the efficacy of the ISMC controller based on the results obtained from prior simulations and this is what this chapter is about.

4.2 Experimental results and discussions

In order to evaluate and consolidate the previous simulation results, experimental results are carried out on the basis of a test bench existing in the laboratory (LacoSer), as shown in Figure below 4.1 . The list of material used in the experience is given hereafter:

- dSPACE ds1103.
- Voltage and current sensors.
- DC-DC boost converter.
- PV module.

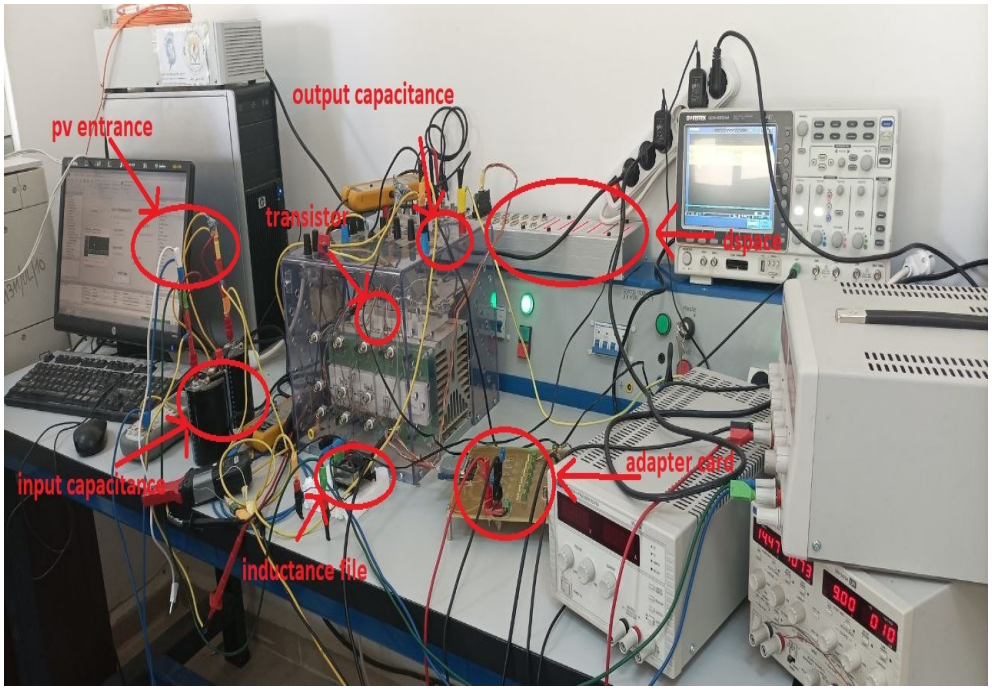

Figure 4.1: Different required devices used for practical experience.

– adaptation cart.

– Graphical User Interface (GUI).

4.3 The devices used in the experiment

Here we gonna talk about the devices used in our experiment

4.3.1 PV panel

The parameter of the panel used are shown in table below (table 4.1) and the pv figure 4.2.

Parameter	Value
Power at MPP Pmpp(W)	**85**
short circuit current Isc(A)	**5.02**
voltage at MPP Vmpp(V)	**29**
current at MPP Impp(A)	**4.76**
open circuit voltage Voc(V)	**22.1**
Nc	**60**

Table 4.1: Parameters of PV Panel

Figure 4.2: The PV panel

4.3.2 dSPACE 1103 Device

The dSPACE 1103 is an advanced and powerful programmable logic controller designed for real-time control and rapid prototyping applications. Equipped with a high-performance processor and a host of I/O interfaces, the ds1103 delivers exceptional computing power and flexibility. It is characterized by precise and deterministic execution, enabling precise control of complex control systems. The device's robust

Parameter	Specifications
Power consumption	5 V; max. 750 mA (via DS1103 board)
Grounding	The enclosure and the front panel are not grounded.
Cable length	2 m (6.6 ft) standard
Physical size (with desktop enclosure) (lengthx depth x height)	647 x 142.5 x 70 mm(25.47 x 5.61 x 2.75 in)
Space needed for 19” rack mount	Height 3 U; width 16.8” + height 3 U; width 8.4”
Weight	Approx. 4.3 kg (9.5 lbs);

Table 4.2: Dspace Data Sheet

construction and reliable operation make it suitable for a wide range of industrial automation and test applications. With its versatile software environment and seamless integration with the comprehensive dSPACE toolkit, the Dspace 1103 provides engineers and researchers with a reliable and efficient platform for developing and validating control algorithms in real-time environments [28].

Figure 4.3: Dspace 1103

The following table 4.2 shows the data sheet of Dspace 1103 Connector/LED Combi Panel

4.3.3 Voltage and current sensors

Voltage sensors

A voltage sensor is a device or component used to measure or detect the electrical potential difference, known as a potentiometer, between two points in an electrical circuit. It is designed to accurately sense and provide an output proportional to the voltage being measured, enabling electrical systems to be monitored, controlled and protected. Voltage sensors play an important role in various applications, such as power distribution, power management systems, renewable energy generation, and industrial automation[29] .

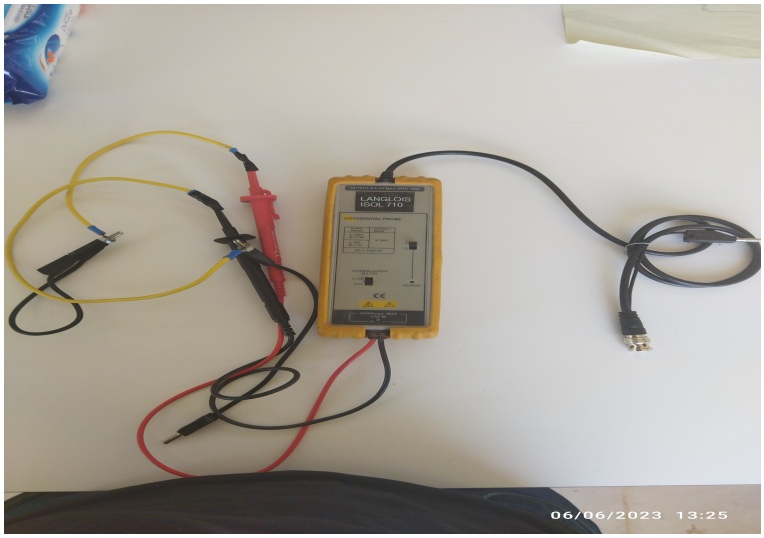

Figure 4.4: Voltage sensor

Current sensor

A current sensor refers to a device or unit used to measure and monitor the flow of electric current in a circuit. Its primary function is to accurately detect and provide an output proportional to the current flowing through a particular conductor or part of the electrical system. Current sensors are essential components in many applications, including power systems, motor control, power monitoring, fault detection, and electronic circuit protection. They enable accurate measurement and control of

current levels, facilitating the efficient and safe operation of electrical equipment and systems[29].

Figure 4.5: Current sensor

4.3.4 DC-DC Boost converter

To build the boost converter, we used the switching and diode controls from the semikron and supplemented them with an external capacitor. This integration allowed us to enhance the functionality and performance of the converter system. By incorporating an external capacitor, we aim to improve energy storage and improve the overall efficiency of the boost converter design.

4.3.5 Adapter card

We have identified that the input voltage requirement for the DC-DC converter is 15V. However, the voltage output from the dSpace system is only 5V. In order to address this discrepancy, our proposed solution involves utilizing an adaptation card to obtain the appropriate voltage level for our needs see figure below (4.8)

we've the schema of the experimental experience(Figure 4.9):

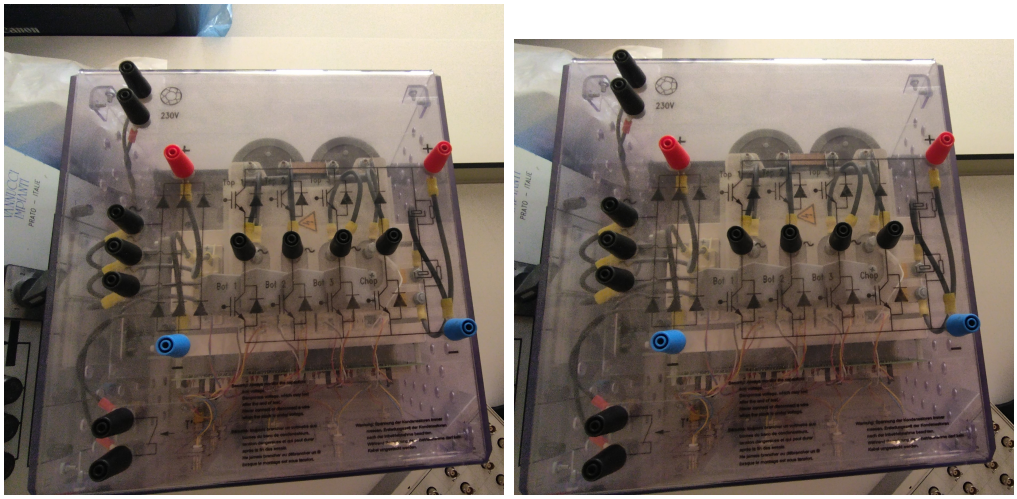

Figure 4.6: The semikron inverter .

Figure 4.7: The external capacitor.

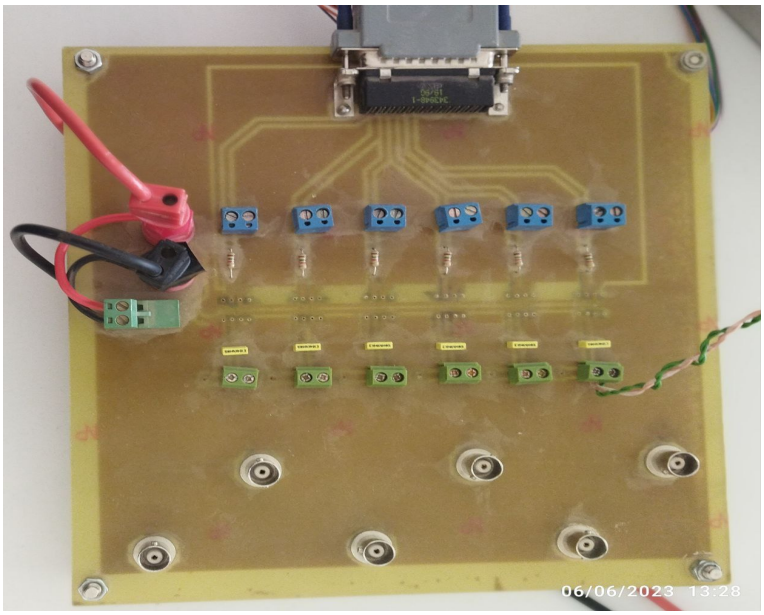

Figure 4.8: Adaptated card

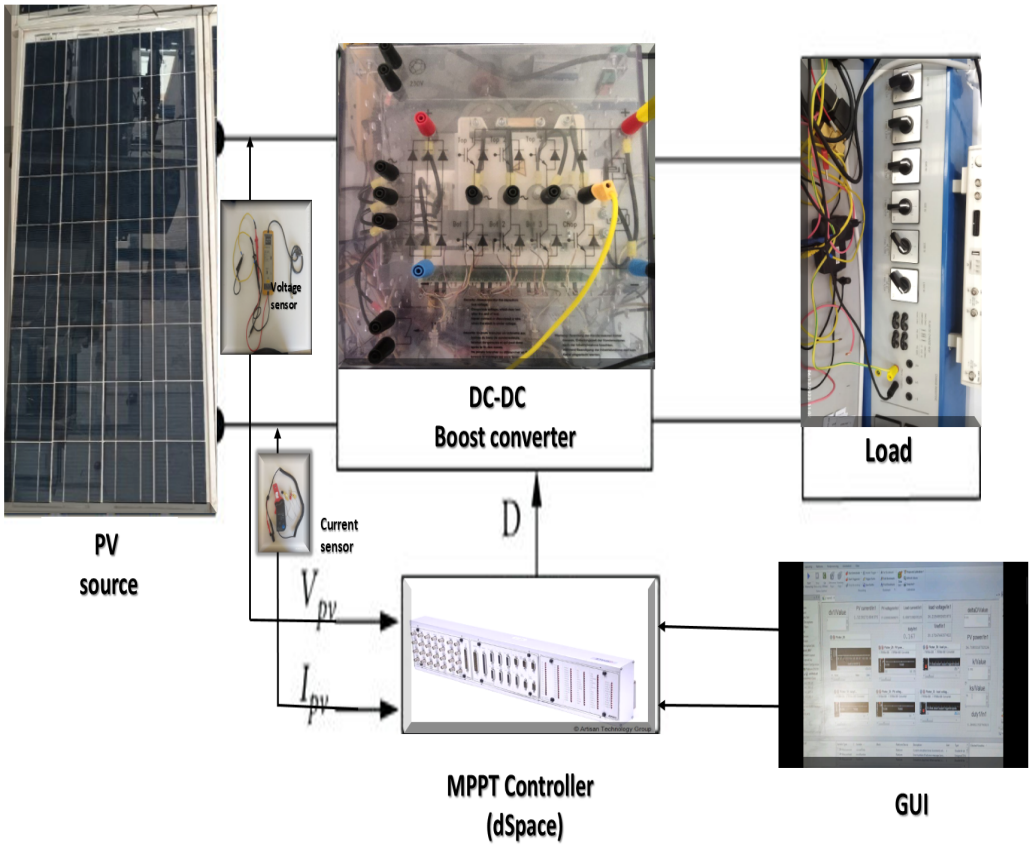

Figure 4.9: The schema of the experimental experience

4.4 Experimental results using the P&O algorithm with and without ISMC

The controller's strategies are applied practically to the PV system. The different experimental PV and load responses are shown in Figures below. The experimental results show that the two different PV responses (PV−voltage, PV−power,) are following practically their MPPT values by applying the two controllers with the same weather practical conditions (irradiation and temperature). However, in the case of the ISMC, the state error and the chattering phenomena are reduced considerably (see Figure 4.14 and 4.15)). As a result, a smooth PV power form (very small chattering level) is achieved by the use of the ISMC (see Figure 4.15). Elsewhere, the experimental load responses are depicted in Figure 4.14 and 4.15. From these results, one can remark that the load responses (load−voltage, load−power) follow their MPPT

required values. In the case of using P&O algorithm see Figure 4.11 and 4.12 all the practical responses contain the chattering phenomena with a non nil state error, but these drawbacks are significantly reduced in the case of ISMC (see Figure 4.14 and 4.15. In fact, a smooth load voltage and power are guaranteed for feeding the load. So, by using the ISMC the power quality is suitably enhanced.

4.5 Experimental results using the controllers

4.5.1 The first Case (installed PV)

The first Case (installed PV) (P&O without ISMC)

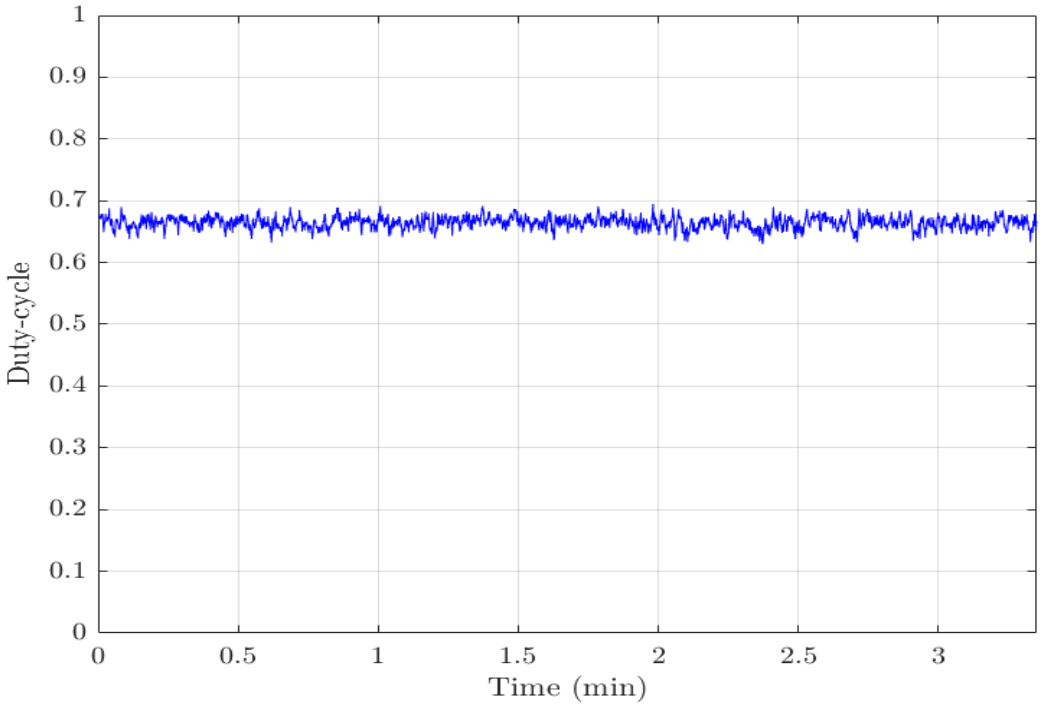

Figure 4.10: Duty cycle

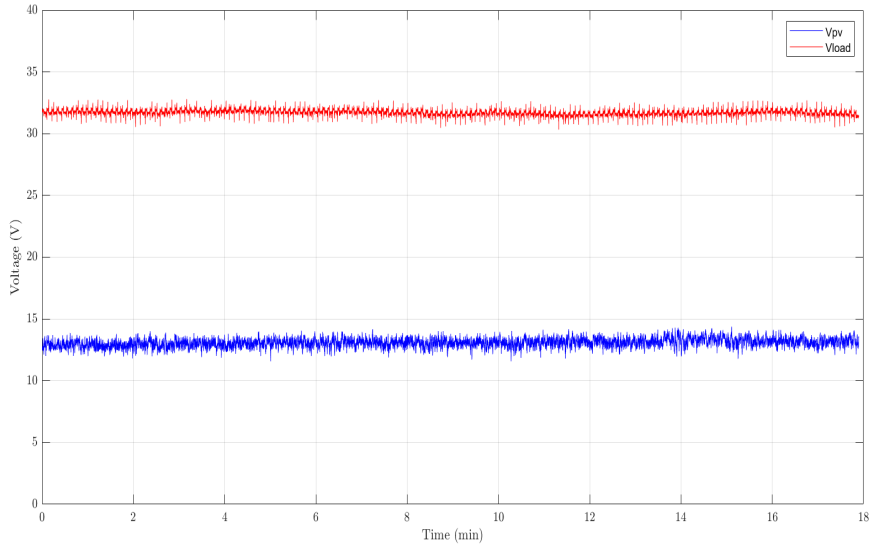

Figure 4.11: The voltage of P&O algorithm without ISMC

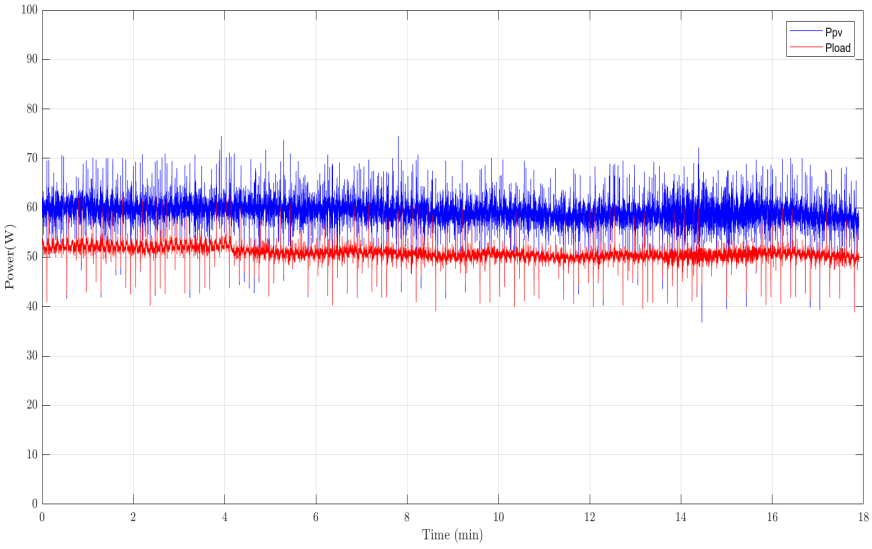

Figure 4.12: The power of P&O algorithm without ISMC

The first Case (installed PV) (P&O with ISMC)

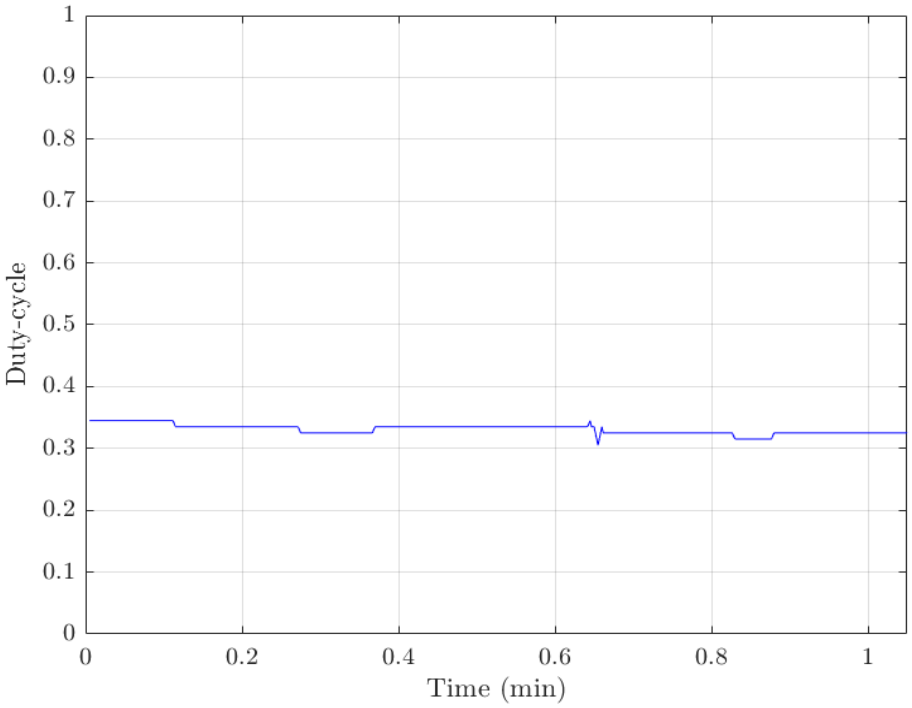

Figure 4.13: Duty cycle

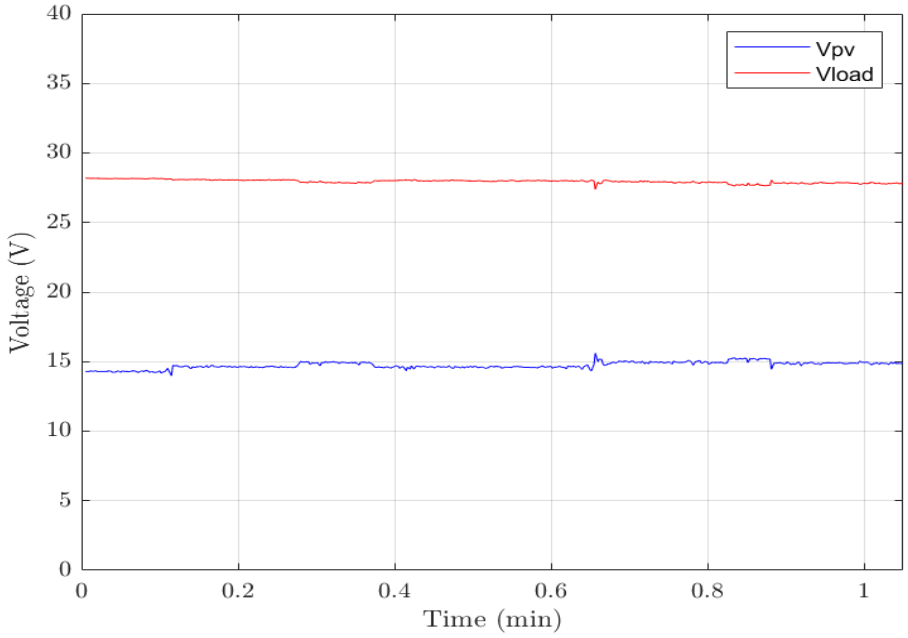

Figure 4.14: The voltage of P&O algorithm with ISMC

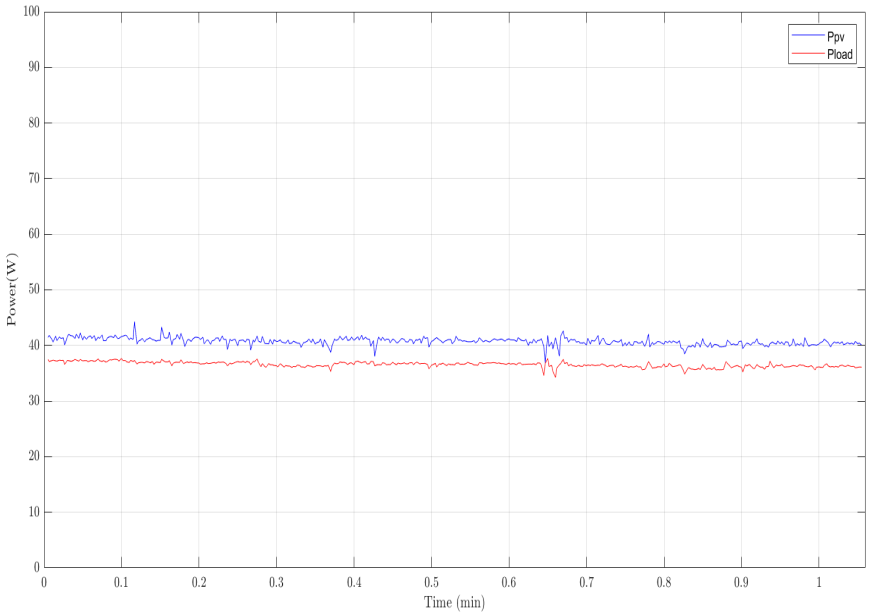

Figure 4.15: The voltage of P&O algorithm with ISMC

4.5.2 The second case Moving the PV panel

In order to test the robustness of global stability and performances (global stability, tracking the reference values) of ISMC, a second test is performed. In fact, the experiments were carried out by considering a large change in PV panel positions. A comparison between P&O with and without ISMC has been made in real-time under the same irradiation and temperature. The obtained experimental results for both controllers are shown in Figure 4.17 and 4.18 and 4.20 and 4.21 From the results it can be seen that the use of ISMC controller allows, a great improvement of the load power quality, a high reduction of the chattering phenomenon and minimized steady state-error.

The second case Moving the PV panel (P&O without ISMC)

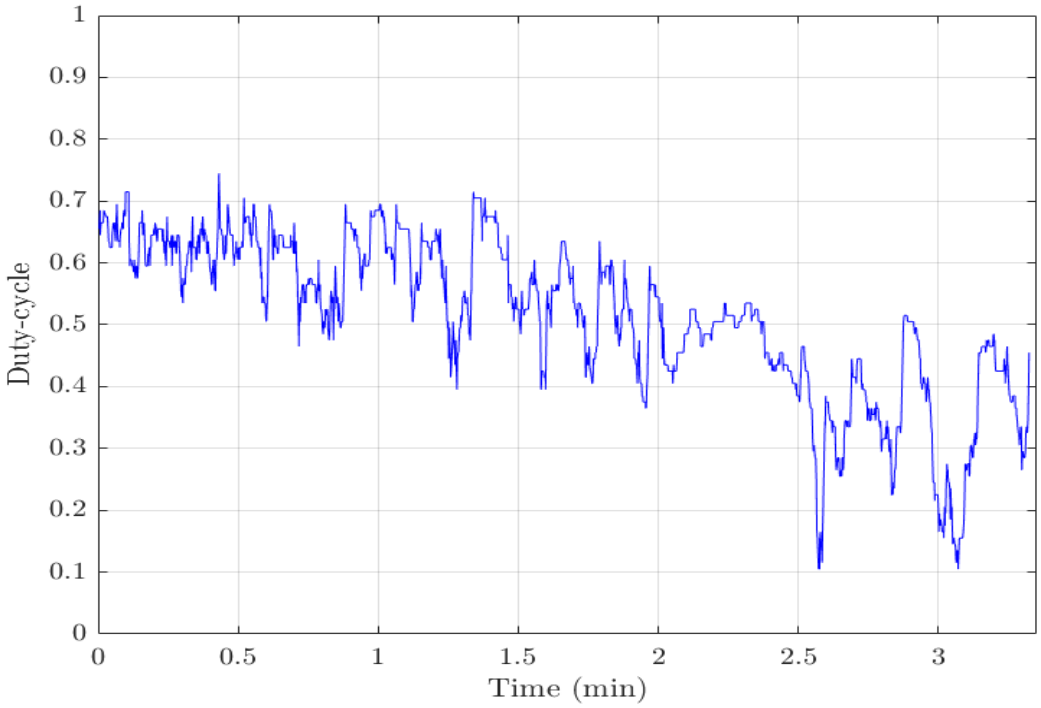

Figure 4.16: Duty cycle

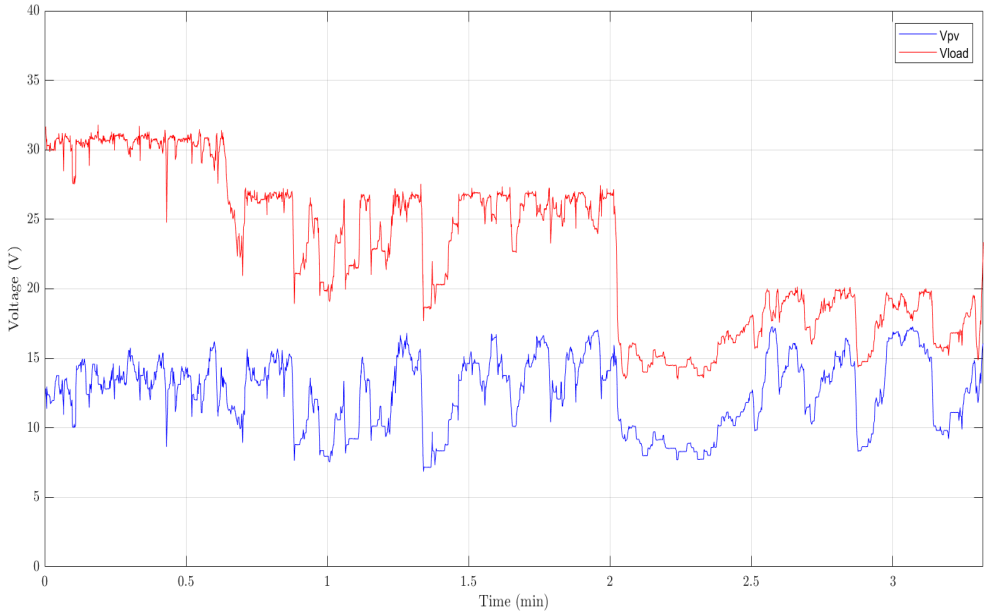

Figure 4.17: The voltage of P&O algorithm without ISMC

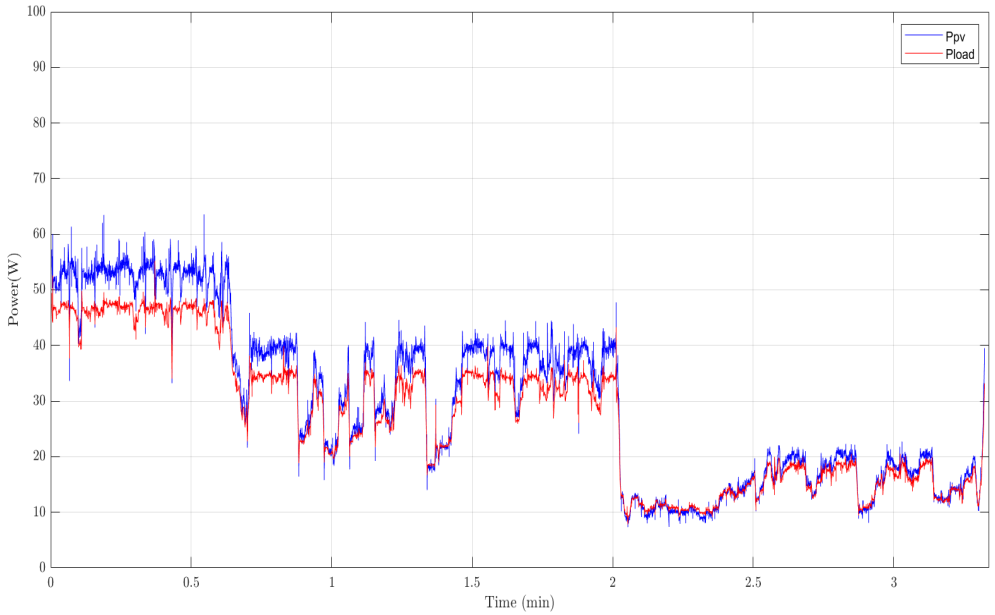

Figure 4.18: The power of P&O algorithm without ISMC

The second case Moving the PV panel (P&O with ISMC)

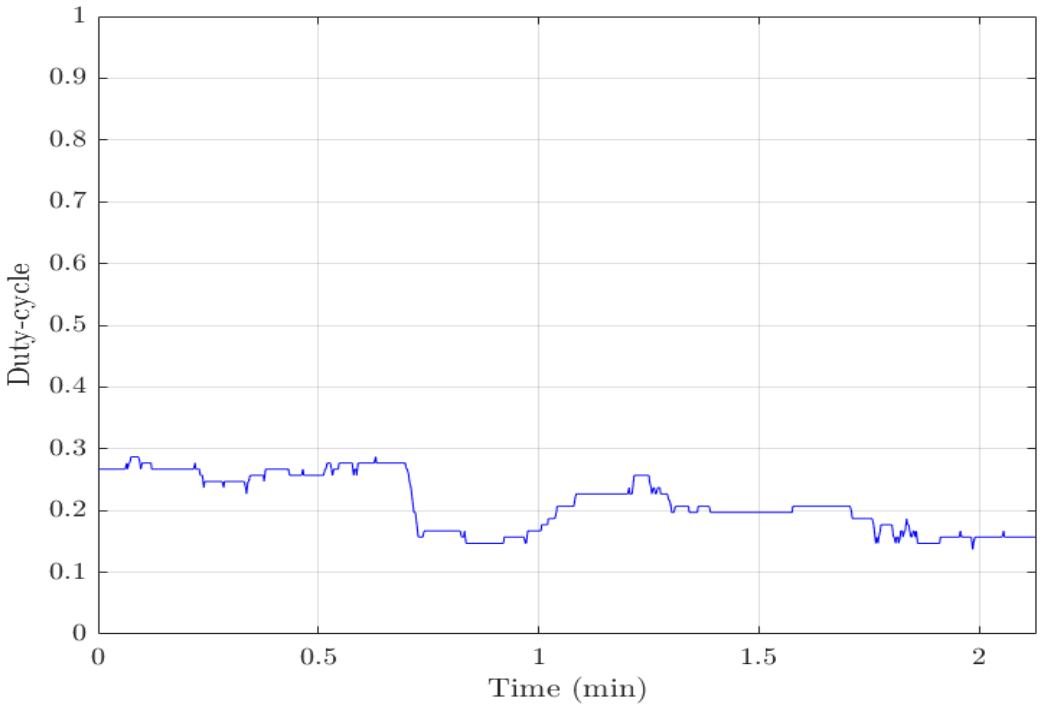

Figure 4.19: Duty cycle

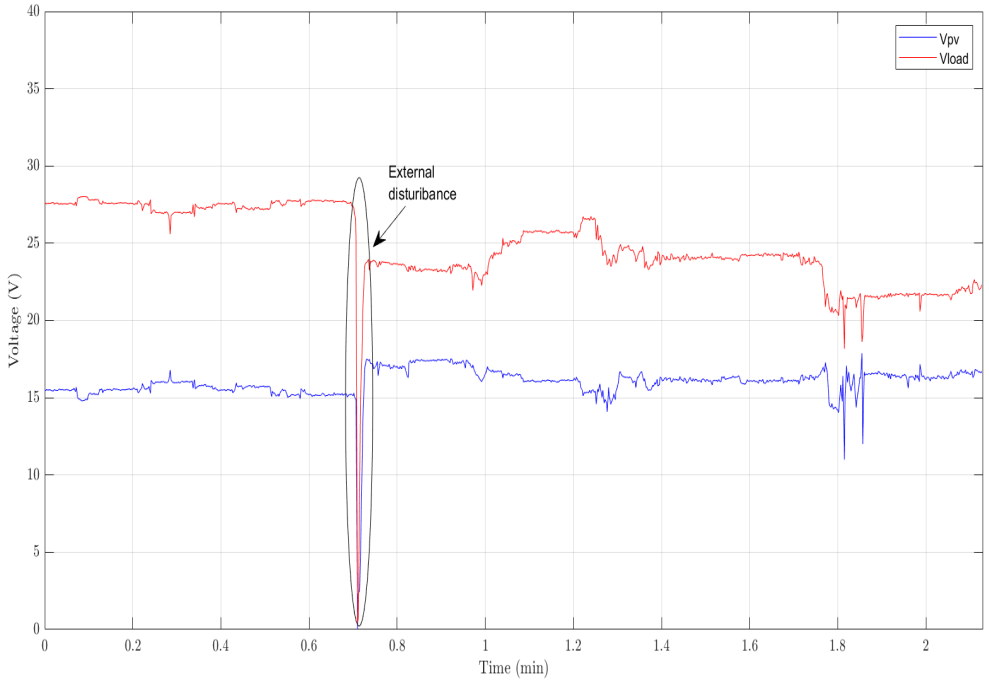

Figure 4.20: The voltage of P&O algorithm with ISMC

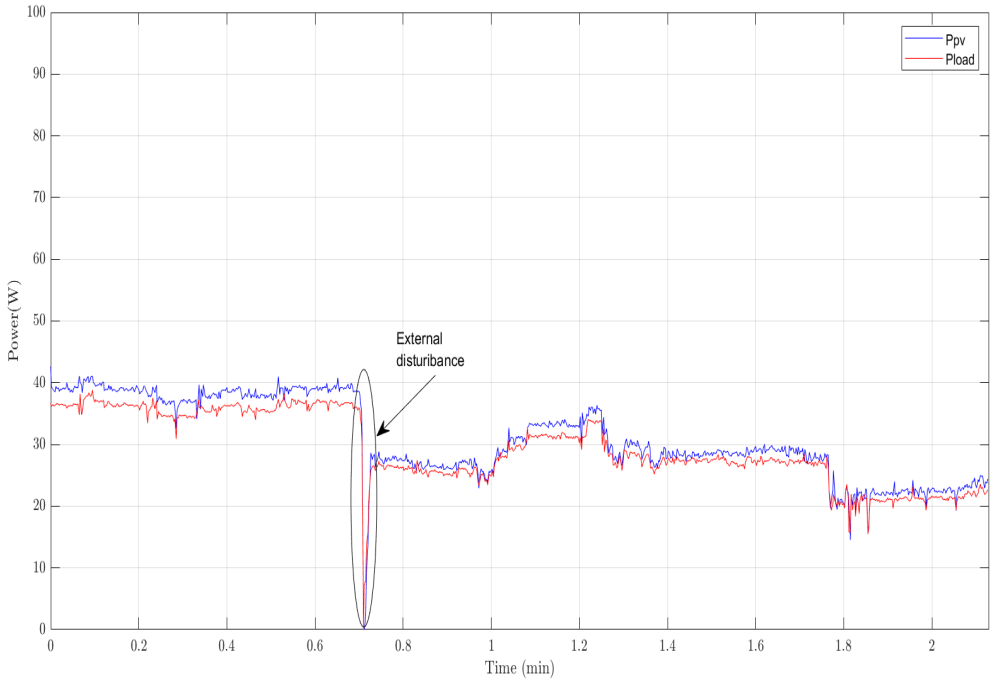

Figure 4.21: The voltage of P&O algorithm with ISMC

4.6 Conclusion

In this chapter, we tested P&O algorithm without and with ISMC to achieve MPP production of a PV system in two cases. In the both cases. The performances of the ISMC have been applied and tested through simulations and experimental validation using a test bench. Furthermore, The performances of the P&O algorithm have been compared experimentally with a nonlinear Integral Sliding mode controller (ISMC). In fact, comparatively to P&O algorithm the ISMC has provide a good performances in terms of chattering phenomena reduction and steady state error elimination. In other words, the obtained experimental result demonstrate an improved steady-state error and chattering phenomena minimization, using the ISMC in both cases (Install and move the PV panel). So, the MPP tracking is accurately achieved in this mode and the system power quality is suitably enhanced.

General Conclusion

In conclusion, this thesis aimed to achieve a nonlinear control strategy to maximize energy extraction from photovoltaic (PV) modules. Through in-depth exploration of solar energy, photovoltaic systems, DC-DC converters, and maximum power point tracking (MPPT) algorithms, great contributions have been made to the field of photovoltaic system optimization.

The research conducted in this thesis highlights the importance of efficient energy extraction from photovoltaic modules and the role of nonlinear control strategies in achieving this goal. Through the development and implementation of a nonlinear control strategy, the thesis demonstrated its potential in enhancing the overall performance and efficiency of PV systems.

The simulation results presented in this thesis show the effectiveness and superiority of the nonlinear control strategy in maximizing the power output. Comparison and analysis of different MPPT algorithms provided valuable insights into their performance under different environmental conditions.

Moreover, the experimental implementation validated the simulation results and highlighted the practical feasibility of the nonlinear control strategy. Through real-world experiments, the thesis bridges the gap between simulation-based research and practical application.

While this thesis has successfully achieved its goals, there are still areas for further exploration and improvement. Future work endeavors could focus on optimizing and enhancing the nonlinear control strategy, considering additional factors such as system stability, network integrity, and cost-effectiveness.

Bibliography

[1] A. Bhatia. Design and Sizing of Solar Photovoltaic Systems. Continuing Education and Development, Inc, 2014.

[2] Sustainable investing - fossil fuel alternatives,accessed 20 april 2023 https://www.robeco.com/en-int/glossary/sustainable-investing/fossil-fuel-alternatives.

[3] Photovoltaic system - energy education, accessed 23 april 2023, https://energyeducation.ca/encyclopedia/photovoltaic system.

[4] HARAOUBIA Mohamed. Intitulé: Etude simulation d'un générateur de panneau photovoltaïque. PhD thesis, UNIVERSITE BADJI MOKHTAR ANNABA, 2019.

[5] Othmane Benseddik and Fathi Djaloud. Etude et optimisation du fonctionnement d'un système photovoltaïque. mémoire de master, université Kasdi Marbah-Ouargala, 2012.

[6] Abdelbassit Zaoui, Abdelhamid Lahbib, Slimane Laribi, et al. Contrôle MPPT basé sur une techniques intelligent pour un système photovoltaïque. PhD thesis, universite Ahmed Draia-ADRAR, 2021.

[7] souid saber, Mecheri Salah Eddine, and Nini Idris. Simulation and realization of mppt methods in photovoltaic system. 2021.

[8] Martin A Green. Solar cells: operating principles, technology, and system applications. Englewood Cliffs, 1982.

[9] Short-circuit-current, accessed 24 april 2023, | PVEducation, https://www.pveducation.org/pvcdrom/solar-cell-operation/short-circuit-current.

[10] Mabrouk Adouane. Etude et conception d'une stratégie de commande d'un onduleur connecté au réseau électrique. PhD thesis, Ecole nationale polytechnique, 2008.

[11] Aissa Bouzid and Messaoud Makhèouf. Etude et optimisation d'un modèle de conversion d'énergie photovoltaique. application au pompage. 2017.

[12] The advantages and disadvantages of solar energy.

[13] Zhour Abada and Malek Bouharkat. Study of management strategy of energy resources in algeria. Energy Reports, 4:1–7, 2018.

[14] Observ'ER - l'observatoire des énergies renouvelables.

[15] Conception, modélisation et réalisation d un système photovoltaïque de moyenne puissance - PDF téléchargement gratuit.

[16] Nabil Abouchabana. Etude d'une nouvelle topologie buck-boost appliquée à un MPPT. PhD thesis, Ecole nationale polytechnique, 2009.

[17] Nouar Aoun and R Chenni. Etude et modélisation des différents modèles de la cellule photovoltaique établkis sur base de valeurs nominales. 2017.

[18] Zainal Salam, Jubaer Ahmed, and Benny S Merugu. The application of soft computing methods for mppt of pv system: A technological and status review. Applied energy, 107:135–148, 2013.

[19] El Kaissa Mehidi. Commande directe par la méthode "Perturb and observe"(P&O) d'un système photovoltaïque. PhD thesis, UNIVERSITE MOULOUD MAMMERI TIZI-OUZOU, 2018.

[20] Cedric Cabal. Optimisation énergétique de l'étage d'adaptation électronique dédié à la conversion photovoltaïque. PhD thesis, Université Paul Sabatier-Toulouse III, 2008.

[21] M Rifa'i and P RatnaIka. Pemodelan dan analisis panel photovoltaik. In Conference Informatic, Telecommunications Electrical Engineering. UGM Yogyakarta, 2012.

[22] T Balamurugan and S Manoharan. Fuzzy controller design using soft switching boost converter for mppt in hybrid system. International Journal of Soft Computing and Engineering, 2(5):87–94, 2012.

[23] Électronique fondamentale a. OUMNAD. a. oumnad - ecole mohammadia d'ingénieurs 1 - PDF téléchargement gratuit.

[24] CHOUTRI Kheireddine, YAHLALI Younes, and Mr BENCHOUBANE Hacine. DEVELOPPEMENT ET IMPLEMENTATION DES ALGORITHMES DE GUIDAGE, NAVIGATION ET DE CONTRÔLE APPLIQUES AUX QUADRI-ROTOR.

[25] SAID Moustafa MOHAMMADI Houssem Eddine. Commandes lineaires et non-lineaires dediees a un uav de type quari-rotor avec tolerance aux default, 2016.

[26] Bellahcene Zakaria. Synthèse de lois de commande robuste pour un hélicoptère à quatre hélices. Université des Sciences et de la Technologie d'Oran Mohamed Boudiaf, le, 6(3), 2013.

[27] Jean-Jacques E Slotine, Weiping Li, et al. Applied nonlinear control, volume 199. Prentice hall Englewood Cliffs, NJ, 1991.

[28] Abdallah Darkawi. Initiation au système dSPACE, de l'interface RTI dans simulink et de ControlDesk next generation 5.4.

[29] Ying Yang and Dongxiang Jiang. An overview of current sensing techniques for power electronic converters. IEEE Transactions on Power Electronics, 24(2):16–28, 2009.